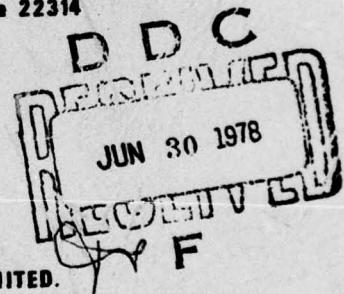SDAC-TR-77-1

THE EFFECT OF CRUSTAL STRUCTURE ON STATION MAGNITUDE ANOMALIES (MAGNITUDE BIAS)

Z.A. Der, T.W. McElfresh & C.P. Mrazek

Seismic Data Analysis Center

Teledyne Geotech, 314 Montgomery Street, Alexandria, Virginia 22314

02 August 1977

78 06 28 124

REPORT DOCUMENTATION PAGE		READ INSTRUCTIONS BEFORE COMPLETING FORM
1. REPORT NUMBER SDAC-TR-77-1	2. GOVT ACCESSION NO.	3. RECIPIENT'S CATALOG NUMBER
4. TITLE (and Subtitle) THE EFFECT OF CRUSTAL STRUCTURE ON STATION MAGNITUDE ANOMALIES (MAGNITUDE BIAS).		5. TYPE OF REPORT & PERIOD COVERED Technical rept, 6. PERFORMING ORG. REPORT NUMBER
7. AUTHOR(s) Zoltan A. Der Thomas W. McElfresh and Charmaine P. Mrazek		8. CONTRACT OR GRANT NUMBER(s) F08606-77-C-0014 ARPA Order - 2551
9. PERFORMING ORGANIZATION NAME AND ADDRESS Teledyne Geotech 314 Montgomery Street Alexandria, Virginia 22314		10. PROGRAM ELEMENT, PROJECT, TASK AREA & WORK UNIT NUMBERS VT/7709
11. CONTROLLING OFFICE NAME AND ADDRESS Defense Advanced Research Projects Agency Nuclear Monitoring Research Office 1400 Wilson Boulevard, Arlington, Virginia 22209		12. REPORT DATE 12 August 1977 13. NUMBER OF PAGES 69
14. MONITORING AGENCY NAME & ADDRESS(If different from Controlling Office) VELA Seismological Center 312 Montgomery Street Alexandria, Virginia 22314	72 p.	15. SECURITY CLASS. (of this report) Unclassified 15a. DECLASSIFICATION DOWNGRADING SCHEDULE

16. DISTRIBUTION STATEMENT (of this Report)

APPROVED FOR PUBLIC RELEASE; DISTRIBUTION UNLIMITED.

17. DISTRIBUTION STATEMENT (of the abstract entered in Block 20, If different from Report)

18. SUPPLEMENTARY NOTES

Author's Report Date 01/14/77

19. KEY WORDS (Continue on reverse side if necessary and identify by block number)

P-waves
Crustal Structure
Body-wave Magnitudes
m_b

20. ABSTRACT (Continue on reverse side if necessary and identify by block number)

The amplification of P wave amplitudes by the receiver crustal structure was modelled for 34 LRSM stations by using crustal structures derived from geological and geophysical information in the literature. Crustal amplification was found to be linearly related to the acoustical impedance in near surface materials at each site. Correlation of the crustal amplification, expressed in magnitude units, with the magnitude residuals of Booth, Marshall and Young (1974) is statistically not significant for the complete set of (Cont'd

DD FORM 1473 EDITION OF 1 NOV 65 IS OBSOLETE
1 JAN 73

stations investigated by the above authors. This indicates that crustal ampli-
fication alone cannot explain the observed magnitude residuals. If two subsets
of stations in Western and Eastern United States, respectively, are taken, a
linear trend between the computed crustal amplification and the magnitude re-
siduals can be seen within each set, but there is a separation of about 0.3
magnitude units between the two groups. The most likely explanation of the
separation is anelastic attenuation in the mantle under the Western United
States. About 75% of variance in the magnitude residuals, for the US stations
used, can be correlated with anelasticity and crustal amplification as known
at present. The residual variance must be due to uncertainties in the above
factors and other causes.

THE EFFECT OF CRUSTAL STRUCTURE ON THE STATION
MAGNITUDE ANOMALIES (MAGNITUDE BIAS)

SEISMIC DATA ANALYSIS CENTER REPORT NO.:   SDAC-TR-77-1

AFTAC Project Authorization No.:   VELA T/6709/B/ETR

Project Title: Seismic Data Analysis Center

ARPA Order No.:   2551

ARPA Program Code No.:   7F10

Name of Contractor: TELEDYNE GEOTECH

Contract No.:   F08606-77-0014

Date of Contract: 01 October 1976

Amount of Contract: $2,674,245

Contract Expiration Date: 30 September 1977

Project Manager: R. R. Blandford
(703) 836-3882

P. O. Box 334, Alexandria, Virginia   22313

ABSTRACT

The amplification of P wave amplitudes by the receiver crustal structure was modelled for 34 LRSM stations by using crustal structures derived from geological and geophysical information in the literature. Crustal amplification was found to be linearly related to the acoustical impedance of near surface materials at each site. Correlation of the crustal amplification, expressed in magnitude units, with the magnitude residuals of Booth, Marshall and Young (1974) is statistically not significant for the complete set of stations investigated by the above authors. This indicates that crustal amplification alone cannot explain the observed magnitude residuals. If two subsets of stations in western and eastern United States, respectively, are taken a linear trend between the computed crustal amplification and the magnitude residuals can be seen within each set, but there is a separation of about .3 magnitude units between the two groups. The most likely explanation of the separation is anelastic attenuation in the mantle under the western United States. About 75% of variance in the magnitude residuals, for the US stations used, can be correlated with anelasticity and crustal amplification as known at present. The residual variance must be due to uncertainties in the above factors and other causes.

TABLE OF CONTENTS

LIST OF FIGURES

LIST OF FIGURES (Continued)

LIST OF FIGURES (Continued)

LIST OF TABLES

INTRODUCTION

Studies of teleseismic magnitude measurements have shown that systematic differences exist between magnitudes observed at various stations which cannot be associated with regional source effects or radiation patterns. The anomalies must, therefore, be associated with the effects of the crust and/or the upper mantle under each station. Booth, Marshall and Young (1974) have published a set of station magnitude corrections, mostly for LRSM stations in North America. The purpose of this study is to evaluate the contribution of crustal structure to the station anomalies. The structure of the North American continent has been studied quite extensively; the crustal structure is reasonably well known at many LRSM stations. At a few stations, however, the structure is not known and at most stations the fine structure is not well known. In such cases a rough model can be obtained by using the regional crustal thicknesses and surface geological information.

We have compiled a set of estimated crustal models for the majority of the stations analyzed by Booth, et al. (1974). In this report we shall compare the crustal magnification computed for each station, based on the assumed models, with the observed magnitude anomalies. The location of stations within the continental U.S. and the short-period residuals are shown in Figure 1.

Booth, Marshall and Young (1974). Long and short-period amplitudes from earthquakes in the range $0^{o}-114^{o}$, Geophys. J. R. Astr. Soc., 39, 523-538.
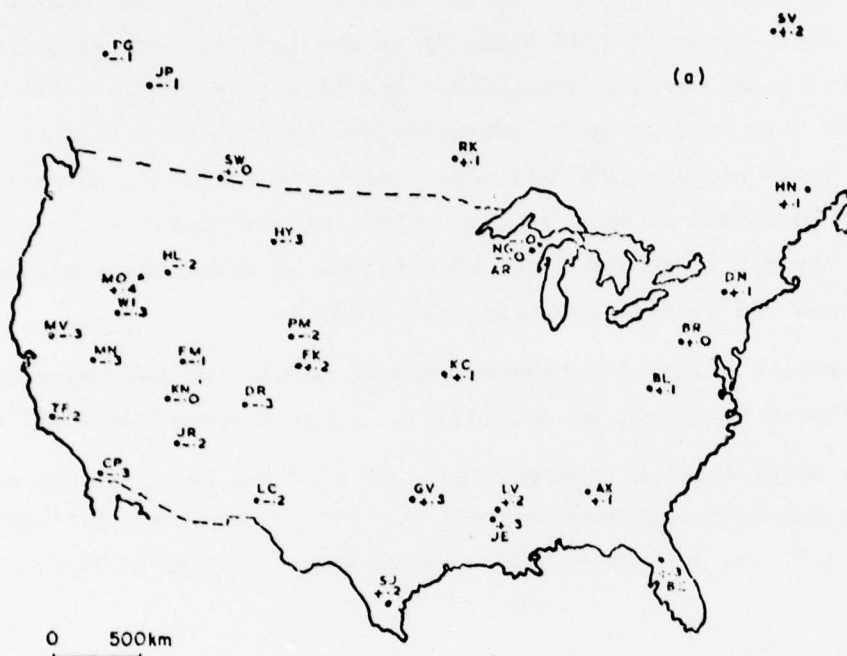
Figure 1.   Short-period magnitude residuals in the United States determined
by Booth, Marshall and Young, 1974.

CRUSTAL MODELS

Since we only want to consider the crust we terminate our models with a halfspace below the Moho. The properties of the local material below the Moho are determined from refraction studies at stations where major refraction surveys are available. At some stations the Geotech LRSM site reports were used to obtain near-surface information. These reports are based on firsthand observations by geologists, together, usually, with perusal of geological maps of the area. Especially important parameters for computing the crustal amplification are the velocities and thicknesses of the unconsolidated sediments near the surface. The lithology by itself is not directly appreciable in this study. Although many previous studies stressed the importance of the nature of the rocks at the surface e.g., Evernden and Clark (1970), such presentations can be very misleading. The velocity of sedimentary rocks is more important than their composition. Some older sedimentary rocks are extremely compact and have high seismic velocities, which are comparable to those of granite and produce amplitudes comparable to granite. On the other hand, thick low velocity sediments can considerably increase the amplitude of seismic waves at the surface.

Crustal models for the set of LRSM stations used are given in Table I. As stated above, these are of varying quality and may be improved as more data becomes available. Besides these, the Geotech LRSM site reports were always considered in constructing the near surface part of each model. Information in these reports varies from quite detailed to sketchy. A considerable amount of information about the near-surface structure has been generated by exploration for oil, but such information is not easily available. There is undoubtedly more information in the general geological literature, but such information is very hard to collect, and the geological literature usually does not give the relevant parameters, the seismic velocities and densities, necessary to construct an accurate geophysical model. The set of models given in this report represents what can be collected with a modest effort from the literature. Quality estimates have been made for each sec-

---

Evernden and Clark, 1970. Study of teleseismic P. II. amplitude data, _Phys. Earth Planet Interiors_, 4, 24-31.

tion. If hard, high-velocity rock is at the surface, the section should be
excellent. Soft rock sites can be excellent if detailed well-logs are
available. If larger thicknesses of the surface soft layer must be guessed,
then the section quality is poor.

TABLE I

Crustal Models for the LRSM Stations in this Study
Section Quality E – Excellent, GF – Good to Fair, P– Poor

STATION (QUALITY)	Layer Thickness d	Compressional Velocity α	Shear Velocity β	Density ρ	SOURCE REFERENCES
AD-IS	6.00	5.50	2.80	2.70	Jacobs and
GF	21.00	6.40	3.60	2.90	Hamada (1972)
	∞	8.10	4.60	3.30	
AR-WS	6.00	5.64	3.47	2.70	Brune and
E	10.50	6.15	3.64	2.80	Dorman (1963)
	18.70	6.60	3.85	2.85	
	∞	8.10	4.72	3.30	
AX-AL	13.00	6.00	3.46	2.70	Antoine and
GF	22.00	6.70	3.89	2.90	Ewing (1963)
	∞	8.10	4.67	3.30	Woolard (1959)
BE-FL	1.00	2.60	1.40	1.80	Antoine and
GF	0.50	3.60	2.00	2.00	Ewing (1963)
	15.00	6.20	3.60	2.80	Woeber and
	17.00	6.70	3.87	2.80	Pennhollow (1975)
	∞	8.10	4.60	3.30	
BL-WV	1.89	6.00	3.46	2.70	Woolard (1959)
GF	25.10	6.15	3.55	2.82	
	9.00	6.58	3.80	2.92	
	∞	8.14	4.76	3.53	
BR-PA	1.89	6.00	3.46	2.70	Woolard (1959)
GF	25.10	6.15	3.55	2.82	
	9.00	6.58	3.80	2.92	
	∞	8.14	4.76	3.53	
CP-CL	4.90	5.80	3.38	2.60	Healy (1973)
E	11.10	6.00	3.50	2.70	Pakiser and
	11.10	7.10	4.00	2.80	Steinhart (1964)
	∞	7.90	4.50	3.30	
DH-NY	1.89	6.00	3.46	2.70	Woolard (1959)
GF	25.10	6.15	3.55	2.82	
	9.00	6.58	3.80	2.92	
	∞	8.14	4.76	3.53	
DR-CO	2.00	6.00	3.42	2.70	Keller, Smith
E	7.00	6.10	3.52	2.70	and Braile (1975)
	15.00	6.40	3.69	2.80	Keller, Smith,
	16.00	6.80	3.92	2.90	Braile, Heaney,
	∞	7.80	4.50	3.30	Shurbet (1976)

TABLE I (Continued)

Crustal Models for the LRSM Stations in this Study
Section Quality E - Excellent, GF - Good to Fair, P - Poor

STATION (QUALITY)	Layer Thickness	Compressional Velocity	Shear Velocity	Density	SOURCE REFERENCES
	d	α	β	ρ	
FK-CO	0.60	2.90	1.55	1.80	Jackson, Steward
GF	0.40	4.80	2.64	2.40	and Pakiser (1963)
	1.30	5.20	3.00	2.60	
	9.90	5.80	3.34	2.70	
	15.50	6.10	3.52	2.80	
	20.00	6.70	3.89	2.90	
	∞	8.00	4.62	3.30	
FM-UT	1.70	3.40	2.00	2.30	Keller, Smith,&
GF	6.70	6.00	3.50	2.80	Braile (1975)
	6.30	5.50	2.90	2.70	Keller, Smith,
	10.00	6.50	3.50	2.80	Braile, Heaney,
	∞	7.40	4.00	3.10	& Shurbet (1976)
GV-TX	1.00	3.05	1.63	1.80	Cram (1961)
E	1.00	4.11	2.26	2.20	Tryggvason &
	1.00	4.42	2.55	2.30	Qualls (1967)
	6.30	5.63	3.24	2.70	
	15.90	6.10	3.52	2.80	
	16.80	6.92	4.00	2.90	
	∞	8.20	4.73	3.40	
HL-ID	8.00	5.20	2.96	2.50	Hill & Pakiser
GF	37.00	6.70	3.82	2.80	(1966)
	∞	7.90	4.50	3.20	
HN-ME	10.00	5.90	3.36	2.70	Dainty, Keen,
GF	20.00	6.35	3.62	2.72	& Blanchard (1966)
	25.00	7.35	4.19	2.83	
	∞	8.10	4.62	3.30	
HW-IS	3.50	3.70	2.11	1.94	Hill (1969)
E	6.50	6.00	3.42	2.70	
	5.00	7.20	4.67	3.40	
	∞	8.20	4.67	3.40	
JE-LA	1.50	2.70	1.44	2.00	Antoine and
E	6.60	3.60	2.00	2.30	Ewing (1963)
	13.00	5.80	3.37	2.70	Woeber and
	15.00	6.70	3.90	2.80	Pennhollow (1975)
	∞	8.10	4.80	3.30	
JR-AZ	0.36	2.50	1.33	1.80	Johnson (1965)
GF	19.00	6.00	3.50	2.70	
	12.00	6.70	3.90	2.80	
	∞	7.90	4.50	3.30	

TABLE I (Continued)

Crustal Models for the LRSM Stations in this Study
Section Quality E - Excellent, GF - Good to Fair, P - Poor

STATION (QUALITY)	Layer Thickness d	Compressional Velocity α	Shear Velocity β	Density ρ	SOURCE REFERENCES
KC-MO	1.94	5.00	2.88	2.60	Stewart (1968)
GF	9.88	6.06	3.50	2.70	
	12.35	6.27	3.62	2.80	
	18.34	6.71	3.87	2.90	
	∞	8.09	4.70	3.30	
KN-UT	2.00	3.15	1.81	2.00	Keller, Smith
GF	7.00	6.10	3.52	2.60	& Braile (1975)
	15.00	6.40	3.69	2.70	Keller, Smith,
	16.00	6.80	3.92	2.80	Braile, Heaney,
	∞	7.80	4.50	3.20	Shurbet (1976)
LC-NM	1.20	3.00	1.60	2.20	Toppozada and
P	5.00	5.80	3.20	2.70	Sanford (1976)
	21.00	6.50	3.80	2.90	
	∞	7.90	4.45	3.30	
LV-LA	1.20	2.70	1.44	2.00	Antoine and
GF	6.00	3.60	2.00	2.30	Ewing (1963)
	13.90	5.80	3.37	2.70	
	15.00	6.70	3.90	2.80	
	∞	8.10	4.80	3.30	
MN-NV	2.00	5.80	3.34	2.50	Hill & Pakiser
GF	27.00	6.15	3.54	2.70	(1966)
	10.00	7.10	4.09	2.90	
	∞	7.80	4.50	3.30	
MO-ID	0.55	1.50	0.75	1.80	Hill & Pakiser
GF	0.43	4.00	2.20	2.50	(1966)
	7.50	5.20	2.97	2.80	(installed in
	37.00	6.70	3.82	2.80	a missile silo
	∞	7.90	4.50	3.20	on silt.)
MV-CL	1.00	3.00	1.60	2.20	Pakiser & Zietz
P	15.00	6.00	3.50	2.70	(1965)
	20.00	6.70	3.90	2.90	
	∞	7.80	4.40	3.30	
NG-WS	6.00	5.64	3.47	2.70	Brune & Dorman
GF	10.50	6.15	3.64	2.80	(1963)
	18.70	6.60	3.85	2.85	
	∞	8.10	4.72	3.30	

TABLE I (Continued)

Crustal Models for the LRSM Stations in this Study
Section Quality E - Excellent, GF - Good to Fair, P - Poor

STATION (QUALITY)	Layer Thickness d	Compressional Velocity α	Shear Velocity β	Density ρ	SOURCE REFERENCES
NP-NT	3.00	4.33	2.50	2.40	Brune & Dorman
GF	9.00	6.00	3.50	2.70	(1963)
	26.00	7.30	4.15	2.90	
	∞	8.20	4.70	3.30	
PG-BC	2.00	5.00	2.90	2.60	White & Savage
P	14.00	6.10	3.50	2.70	(1965)
	14.00	6.70	3.84	2.80	
	∞	8.00	4.60	3.30	
RK-ON	6.00	5.64	3.47	2.70	Brune & Dorman
E	10.50	6.15	3.64	2.80	(1963)
	18.70	6.60	3.85	2.85	
	∞	8.10	4.72	3.30	
SJ-TX	1.00	2.13	1.13	1.80	Woeber &
E	5.30	3.35	1.82	2.00	Pennhollow (1975)
	1.70	3.60	2.07	2.40	
	11.00	6.00	3.46	2.70	
	11.00	6.70	3.87	2.90	
	∞	8.00	4.62	3.30	
SV-QB	1.13	5.80	3.36	2.60	Brune & Dorman
E	20.00	6.20	3.60	2.70	(1963)
	16.00	6.70	3.90	2.90	
	∞	8.00	4.60	3.30	
SM-MA	4.70	5.00	2.85	2.50	Asada & Aldrich
GF	12.00	6.20	3.53	2.70	(1966)
	39.00	6.70	3.82	2.80	
	∞	8.00	4.56	3.30	
TF-CL	2.00	3.00	1.61	2.00	Healy (1973)
P	14.72	6.10	3.52	2.70	Pakiser & Zietz
	9.40	7.00	4.04	2.90	(1965)
	∞	8.10	4.67	3.30	
WH-YK	35.00	6.20	3.54	2.75	LeBlanc &
P	∞	8.20	4.75	3.30	Wetmiller (1974)
WI-NV	3.00	4.50	2.57	2.30	
GF	18.00	6.00	3.42	2.70	
	12.00	6.70	3.82	2.80	
	∞	7.90	4.50	3.20	

COMPUTATIONS

The crustal amplification is a function of not only the material property distribution but also of the angle of incidence. We evaluated the ground amplification for three different pulse shapes using an angle of incidence of 25° below the Moho, which is fairly typical for teleseismic arrivals. The first pulse is chosen to represent the wide-band signal generated by a 5 kt nuclear explosion in granite as seen through the standard LRSM short-period instrument (SP5), the second is a 50 kt explosion seen through the same instrument (SP50) and the third is the 50 kt explosion seen through the LRSM long-period instrument (LP50).

At first we performed exploratory calculations and found that the amplification is relatively insensitive to the moderate variations of the angles of incidence expected for the teleseismic distance range. As we shall see in detail in this report the amplification was also found to be almost as well predicted by the elastic properties of materials near the surface as by the detailed variations of the crustal frequency response with frequency. The dominant period of the transmitted pulses was also found, by visual inspection, to be insensitive to crustal structure. Anticipating results to come, comparison of the amplitudes of station pairs whose structures differed by 5-10% e.g., ADIS-AXAL, ARWS-AXAL, LCNM-MVCL, DHNY-DRCO, NPNT-WINV; reveals magnitude differences ranging from .01 to .05. Thus, we feel that these crustal models are about as accurate as needed for the purposes of estimating magnitudes since most of the structures should be good to 10%. Variations due to focussing should introduce more variance than should inaccruate plane-layer parameters.

The algorithm to compute crustal amplification is the well-known Haskell matrix method (Haskell, 1962) for laterally homogeneous elastic layered media. No anelastic effects in the crust were considered. We assume a dilatational strain amplitude ($\Theta = \frac{\partial u}{\partial x} + \frac{\partial v}{\partial y} + \frac{\partial w}{\partial z}$, where u, v, w are the components of displacement) of unity, in Haskell's notation $\Delta'' = 1$, for the incident wave at the base of our model. This amounts only to a convenient normalization of the incident amplitude. To equalize the elastic energy flux at the base of the model the results of computation have to be divided by $(\rho_n \alpha_n{}^3)^{1/2}$ where

---

Haskell, 1962. Crustal reflection of P and SV waves, J. Geophys. Res., 67, 4751-4767.

ρ_n and α_n are the density and P wave celocity in the sub-Moho halfspace terminating the model. This correction factor can easily be derived from Haskell's equations as given by Båth (1968, p. 282-283) and Ewing, Jardetzky, and Press (1957, p. 28). Figure la shows the location of LRSM stations used within North America.

Figures 2 to 30 show the crustal frequency responses, plotted as power spectra, of the impulse response of the crust; time domain crustal impulse responses, and final pulse shapes for each model and assumed pulse type. The LRSM station in question is indicated at the top of each figure. Below this, the crustal response is shown as a function of frequency between 0-6 Hz. The short-period and long-period impulse responses, and synthetic seismograms are shown below these with the appropriate time scales. All plots are normalized to the same amplitude and the normalizing factors are written beside each plot. Signals which seem to be precursors should, in reality, follow the first main pulse and were created by the "wraparound" affect of the Finite Fourier transform. The effect of these on the logarithms of the main pulse is negligible since they are, in all cases, very small. The maximum amplitude is picked by the computer and printed on the plot. Only the relative changes of amplitude for a fixed pulse type are significant, not the absolute value.

The receiver crust frequency responses show rapid fluctuation with frequency, but averages over wider frequency ranges are approximately constant in spite of the fact that the power is plotted which tends to emphasize the fluctuations on the linear scales employed. In the overwhelming majority of the cases presented, the effect of crustal responses in the estimation of Q by fitting straight lines to spectral ratios would seem to be negligible, since there is no clear trend with increasing frequency. The few exceptions (such as FKCO) serve to demonstrate that crustal responses can, in some cases, contribute to the scatter in Q measurements.
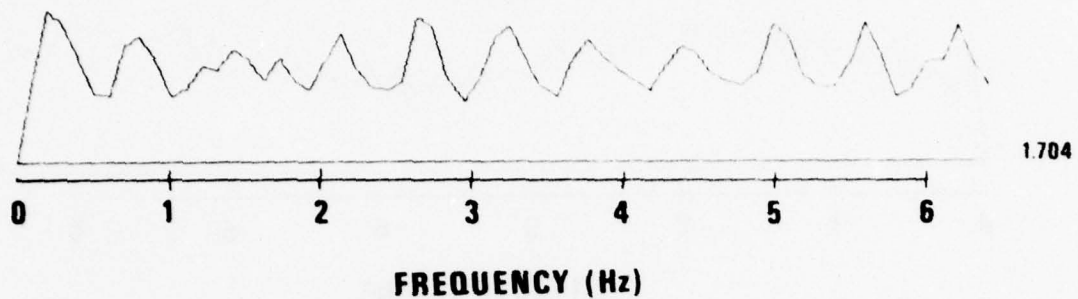
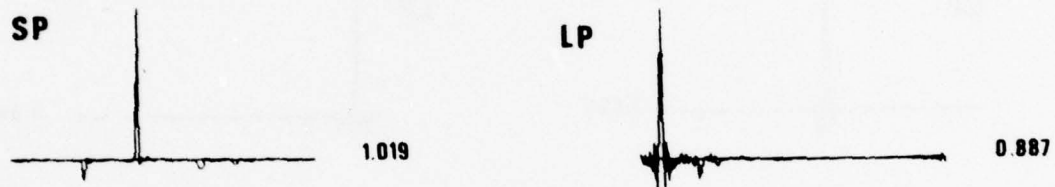Bath, Marcus (1968). Mathematical aspects of seismology, Elsevier Publishing Company, Amsterdam.

Ewing, M. W., Jardetzky, W. S., and F. Press (1957). Elastic waves in layered media. McGraw-Hill Book Co., New York, NY

AD-IS

CRUSTAL RESPONSE

1.704

FREQUENCY (Hz)

CRUST IMPULSE RESPONSE

SP   LP

1.019   0.887

SEISMOGRAMS

5 Kt   50 Kt   50 Kt

20.411   15.009   0.007

SP5   SP50   LP50

0   5   10   0   32   64

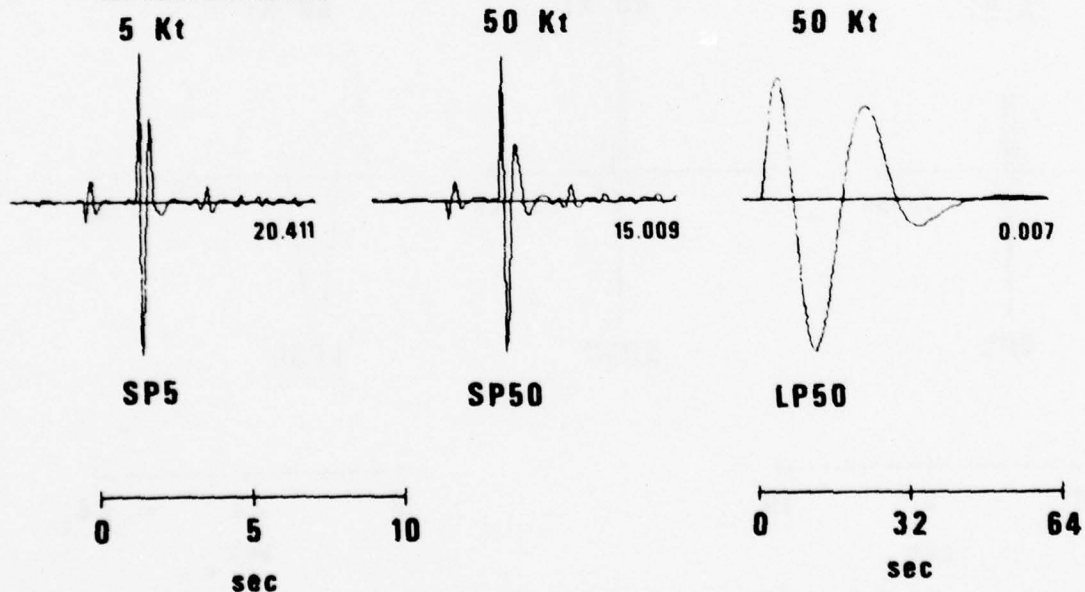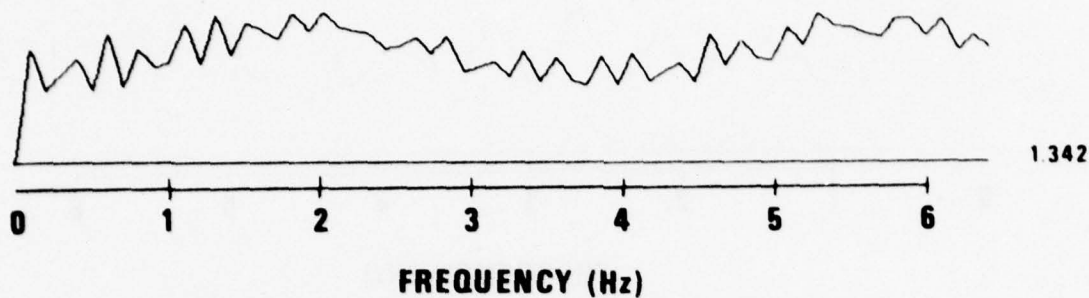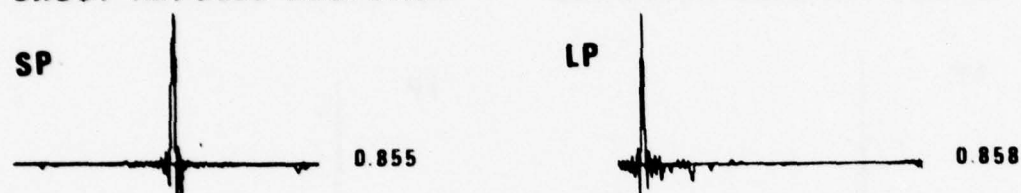sec   sec

Figure 2.   Crustal frequency response function, shown as linear power spectrum
            of the receiver crustal impulse response, receiver crust impulse
            responses, synthetic seismograms for the LRSM station AD–IS.   The
            numbers to the right of abscissa indicate the maximum power or
            amplitude as appropriate.

AX-AL

CRUSTAL RESPONSE

1 342

0   1   2   3   4   5   6

FREQUENCY (Hz)

CRUST IMPULSE RESPONSE

SP   LP

0.855   0.858

SEISMOGRAMS

5 Kt   50 Kt   50 Kt

24.160   14.105   0.007

SP5   SP50   LP50

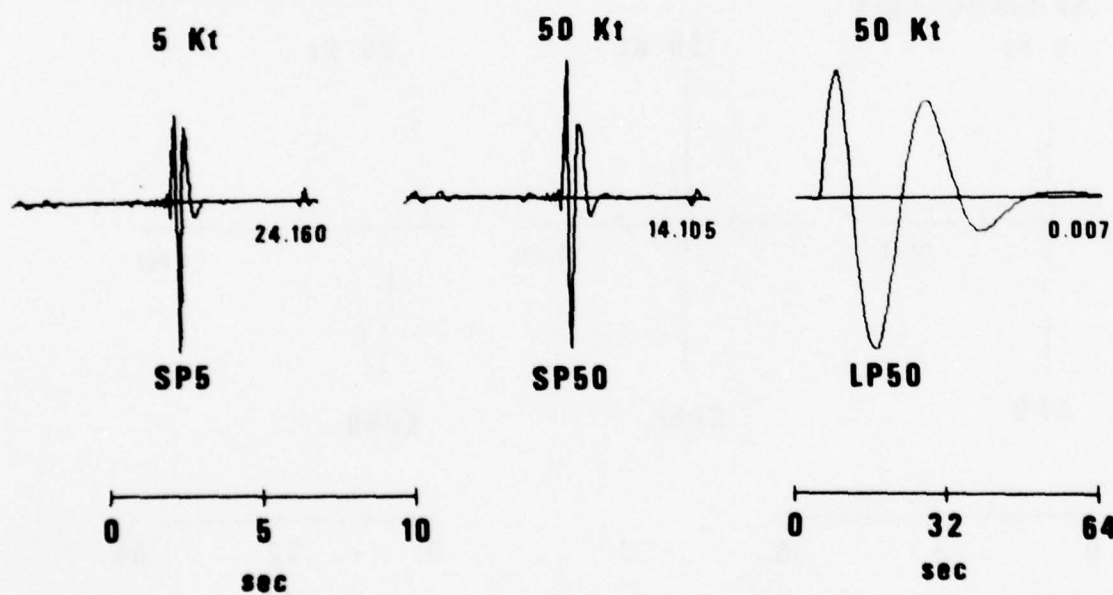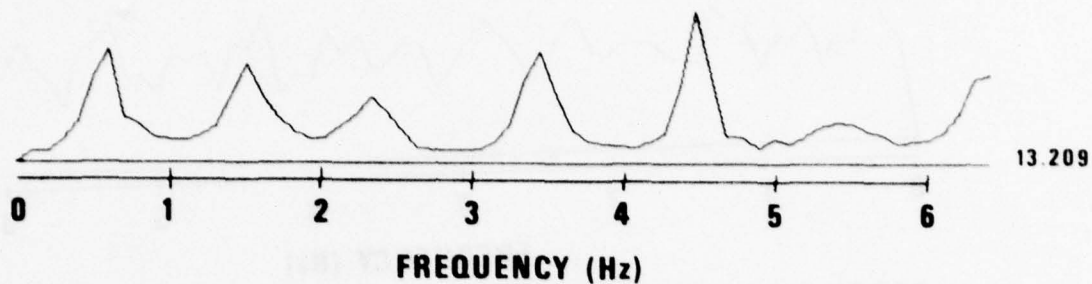0   5   10   0   32   64

sec   sec

Figure 3. Crustal frequency response function, shown as linear power spectrum of the receiver crustal impulse response, receiver crust impulse responses, synthetic seismograms for the LRSM station AX-AL. The numbers to the right of abscissa indicate the maximum power or amplitude as appropriate.
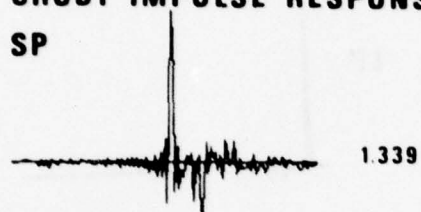
BE-FL

CRUSTAL RESPONSE

13.209

FREQUENCY (Hz)

CRUST IMPULSE RESPONSE

SP

1.339

LP

1.245

SEISMOGRAMS

5 Kt

43.714

SP5

50 Kt

22.053

SP50

50 Kt

0.007

LP50

0   5   10

sec

0   32   64

sec

Figure 4. Crustal frequency response function, shown as linear power spectrum of the receiver crustal impulse response, receiver crust impulse responses, synthetic seismograms for the LRSM station BE-FL. The numbers to the right of abscissa indicate the maximum power or amplitude as appropriate.

CP-CL

CRUSTAL RESPONSE

1.497

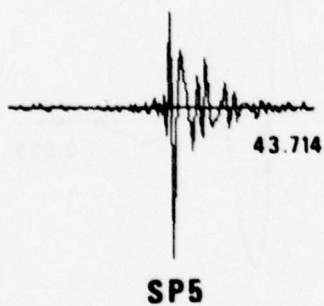### FREQUENCY (Hz)
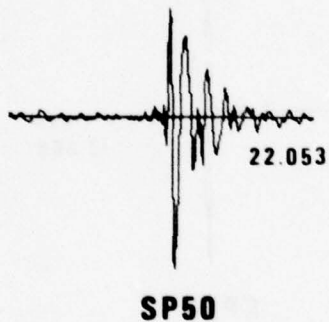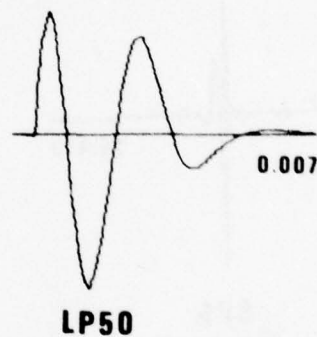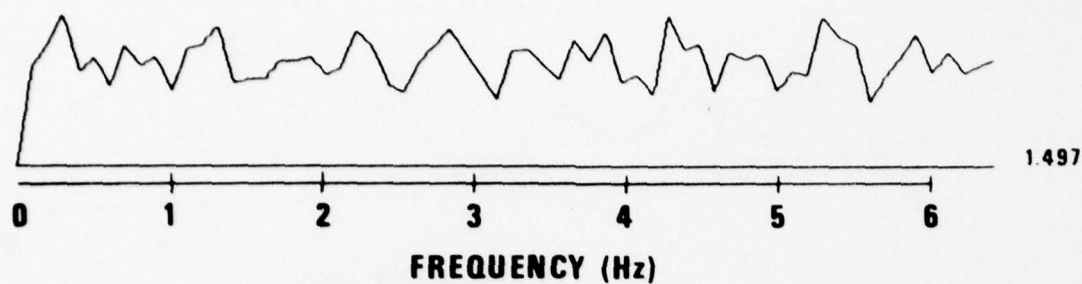
CRUST IMPULSE RESPONSE

SP   LP

0.927   0.996

SEISMOGRAMS

5 Kt   50 Kt   50 Kt

25.479   13.668   0.008
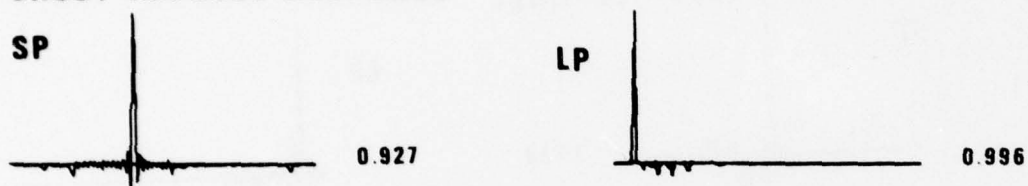
SP5   SP50   LP50

Figure 5. Crustal frequency response function, shown as linear power spectrum
of the receiver crustal impulse response, receiver crust impulse
responses, synthetic seismograms for the LRSM station CP-CL. The
numbers to the right of abscissa indicate the maximum power or
amplitude as appropriate.

-24-

BL-WV
BR-PA
DH-NY

CRUSTAL RESPONSE

1.673

0   1   2   3   4   5   6

FREQUENCY (Hz)

CRUST IMPULSE RESPONSE

SP

0.937

LP

0.991

SEISMOGRAMS

5 Kt

23.103

SP5

50 Kt

14.734

SP50

50 Kt

0.007

LP50

0   5   10
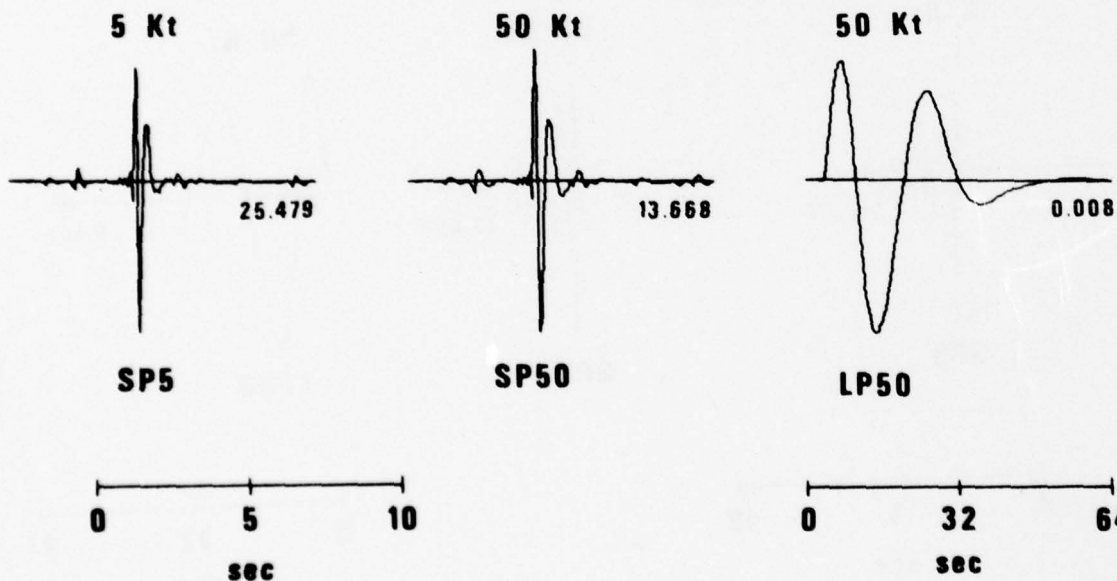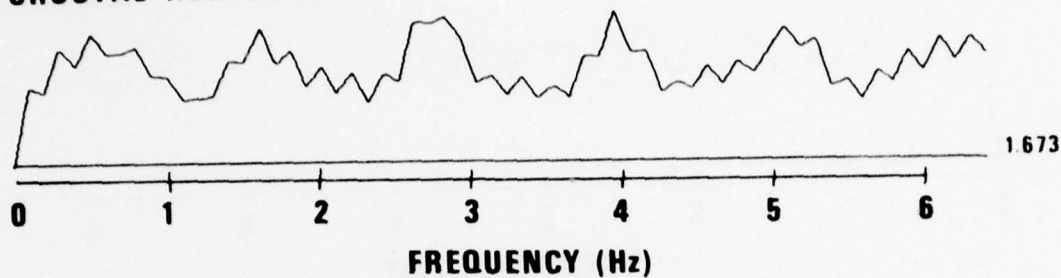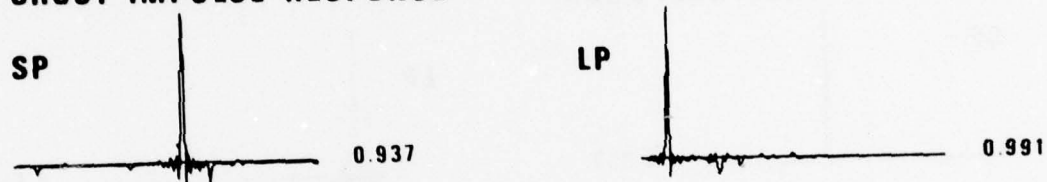**sec**

0   32   64
sec

Figure 6.   Crustal frequency response function, shown as linear power spectrum
of the receiver crustal impulse response, receiver crust impulse
responses, synthetic seismograms for the LRSM station BL-WV, BR-PA
and DH-NY.   The numbers to the right of abscissa indicate the max-
imum power or amplitude as appropriate.

-25-

DR-CO

CRUSTAL RESPONSE

1.355

0   1   2   3   4   5   6

FREQUENCY (Hz)

CRUST IMPULSE RESPONSE

SP

0.963

LP

0.688

SEISMOGRAMS

5 Kt

20.843

SP5

50 Kt

14.129

SP50

50 Kt

0.007

LP50

0   5   10
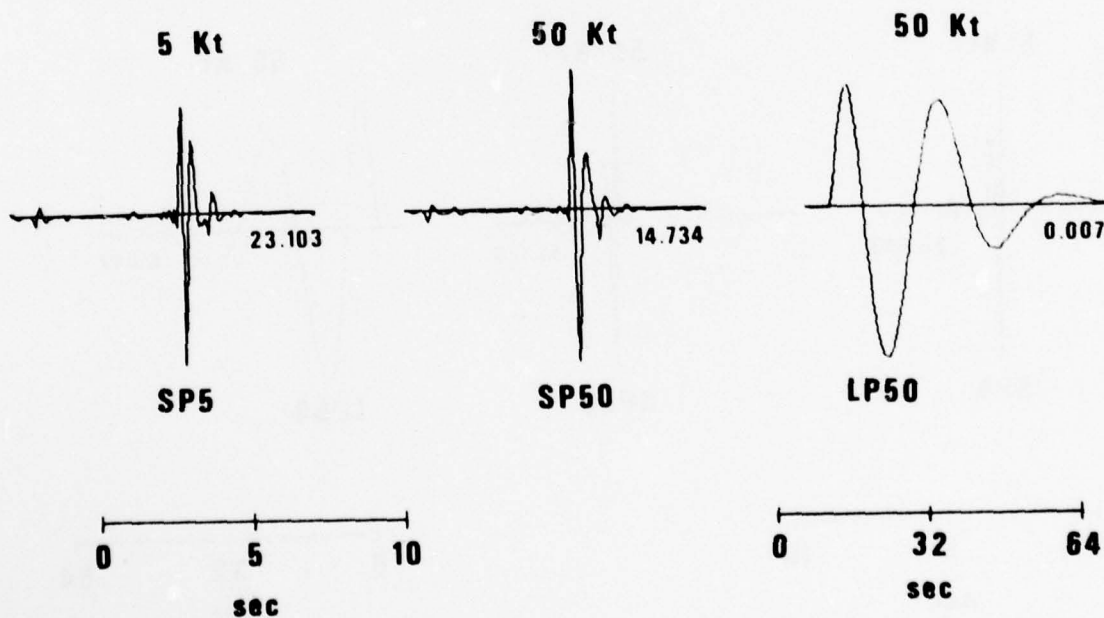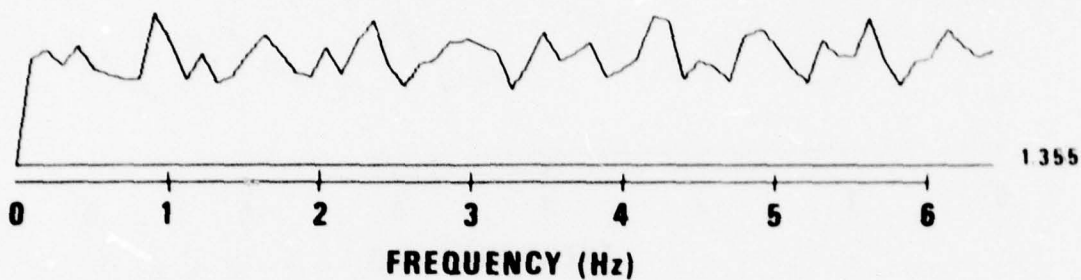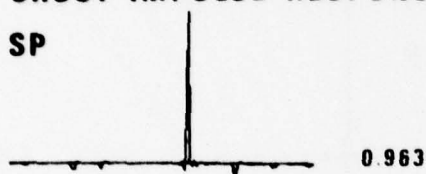
sec

0   32   64

sec

Figure 7. Crustal frequency response function, shown as linear power spectrum of the receiver crustal impulse response, receiver crust impulse responses, synthetic seismograms for the LRSM station DR-CO. The numbers to the right of abscissa indicate the maximum power or amplitude as appropriate.
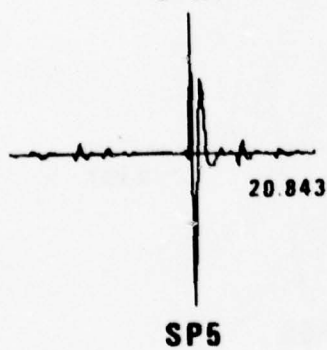
FK-CO

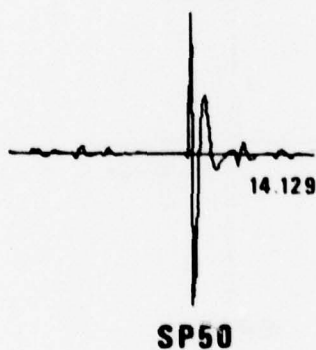**CRUSTAL RESPONSE**

FREQUENCY (Hz)

CRUST IMPULSE RESPONSE

SP

LP

1.625

0.862

SEISMOGRAMS

5 Kt

50 Kt

50 Kt
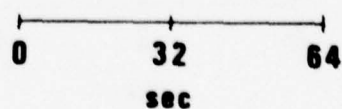
34.551

22.761

0.007

SP5
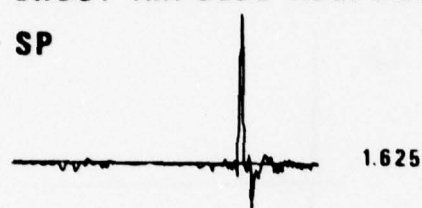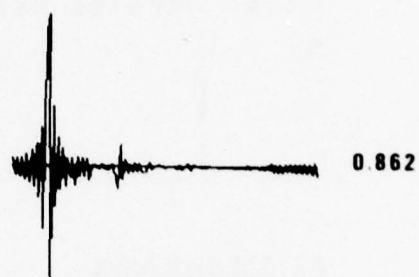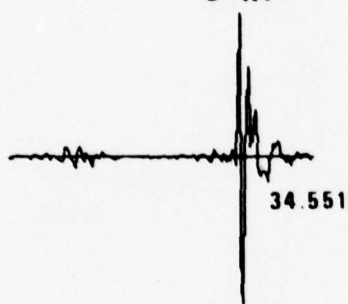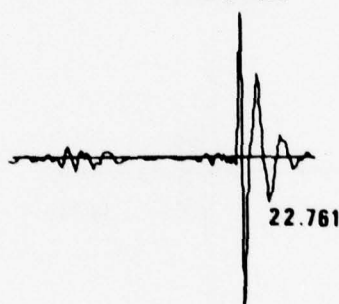
SP50

LP50

Figure 8. Crustal frequency response function, shown as linear power spectrum of the receiver crustal impulse response, receiver crust impulse responses, synthetic seismograms for the LRSM station FK-CO. The numbers to the right of abscissa indicate the maximum power or amplitude as appropriate.

FM-UT

CRUSTAL RESPONSE

4.957

FREQUENCY (Hz)

CRUST IMPULSE RESPONSE

SP

1.192

LP

1.180

SEISMOGRAMS

5 Kt

23.567

SP5

50 Kt

18.138

SP50

50 Kt

0.007

LP50

0   5   10
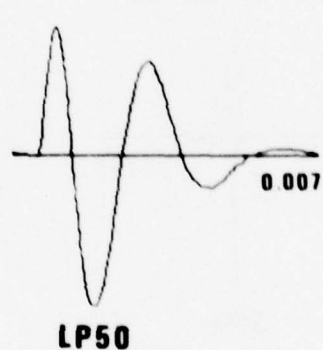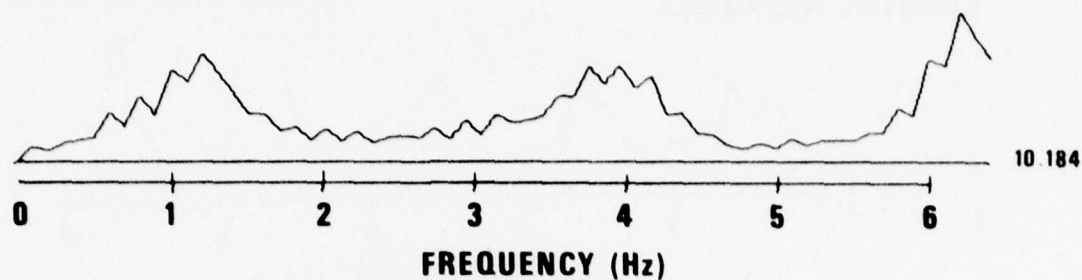sec

0   32   64
sec

Figure 9. Crustal frequency response function, shown as linear power spectrum of the receiver crustal impulse response, receiver crust impulse responses, synthetic seismograms for the LRSM station FM-UT. The numbers to the right of abscissa indicate the maximum power or amplitude as appropriate.

GV-TX

CRUSTAL RESPONSE

8.334

FREQUENCY (Hz)

CRUST IMPULSE RESPONSE

SP

1.167 . 167

LP

1.675

SEISMOGRAMS

5 Kt
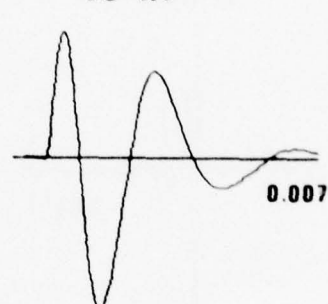

45.344

SP5

50 Kt

21.934

SP50

50 Kt

0.008

LP50

Figure 10. Crustal frequency response function, shown as linear power spectrum of the receiver crustal impulse response, receiver crust impulse responses, synthetic seismograms for the LRSM station GV-TX. The numbers to the right of abscissa indicate the maximum power or amplitude as appropriate.

-29-

HL-ID

CRUSTAL RESPONSE

1.771

0   1   2   3   4   5   6

FREQUENCY (Hz)

CRUST IMPULSE RESPONSE

SP   **LP**

1.034   0.925

SEISMOGRAMS

5 Kt   **50 Kt**   **50 Kt**

20.509   15.421   0.007

SP5   **SP50**   **LP50**

0   5   10   0   32   64

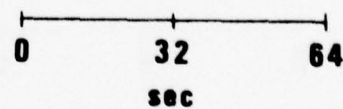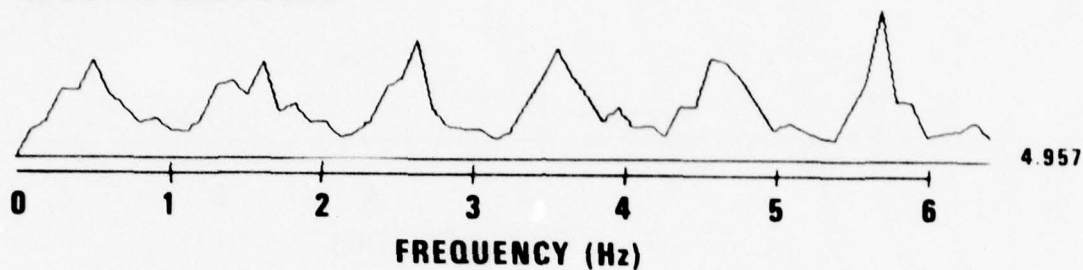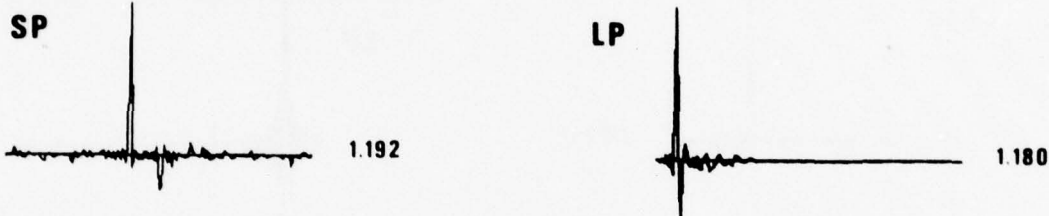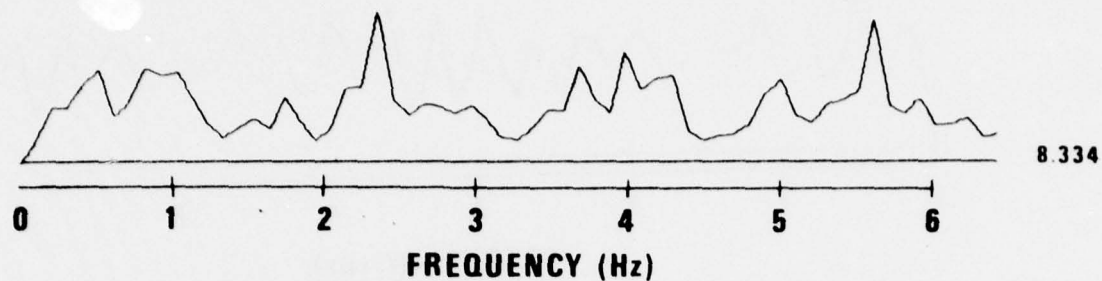sec   sec
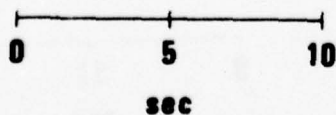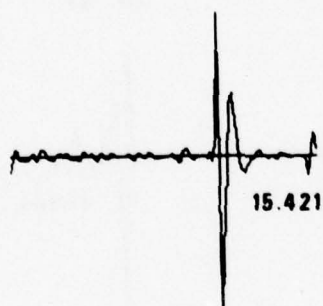
Figure 11. Crustal frequency response function, shown as linear power spectrum
of the receiver crustal impulse response, receiver crust impulse
responses, synthetic seismograms for the LRSM station HL-ID. The
numbers to the right of abscissa indicate the maximum power or
amplitude as appropriate.

-30-

HN-ME

CRUSTAL RESPONSE

1.410

FREQUENCY (Hz)

CRUST IMPULSE RESPONSE

SP

0.968

LP

0.687

SEISMOGRAMS

5 Kt

19.788

SP5

50 Kt

14.562

SP50

50 Kt

0.007

LP50

0   5   10

sec

0   32   64

sec
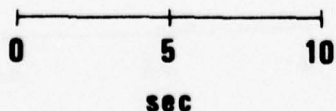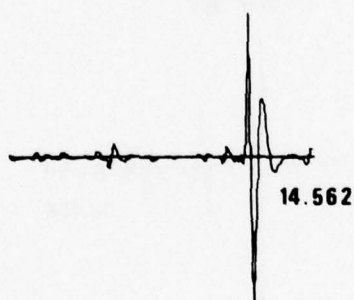
Figure 12.   Crustal frequency response function, shown as linear power spectrum of the receiver crustal impulse response, receiver crust impulse responses, synthetic seismograms for the LRSM station HN-ME. The numbers to the right of abscissa indicate the maximum power or amplitude as appropriate.
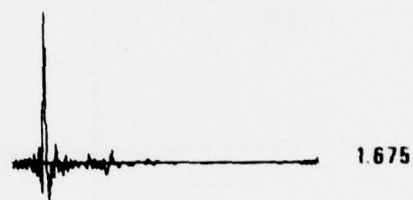
HW-IS

CRUSTAL RESPONSE

FREQUENCY (Hz)

CRUST IMPULSE RESPONSE

SP
1.168

LP
1.310

SEISMOGRAMS

5 Kt
37.456

50 Kt
18.108

50 Kt
0.007
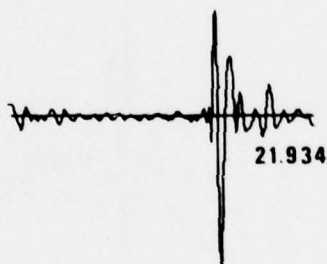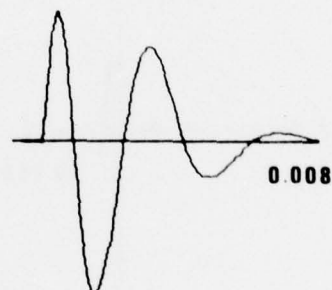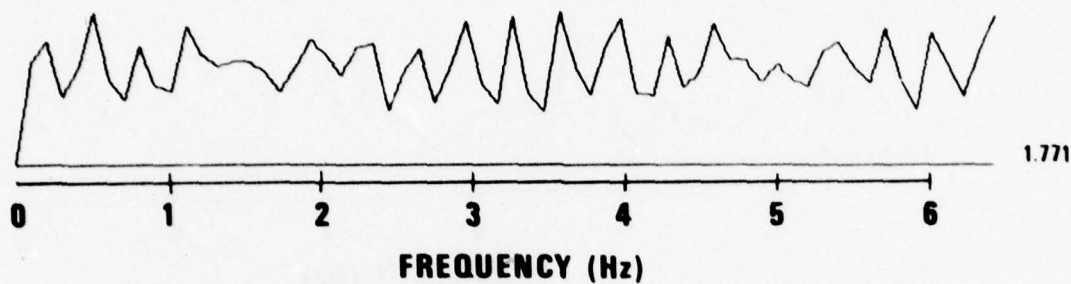
SP5

SP50

LP50

Figure 13. Crustal frequency response function, shown as linear power spectrum of the receiver crustal impulse response, receiver crust impulse responses, synthetic seismograms for the LRSM station HW-IS. The numbers to the right of abscissa indicate the maximum power or amplitude as appropriate.
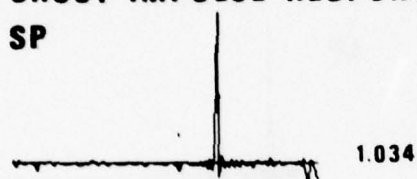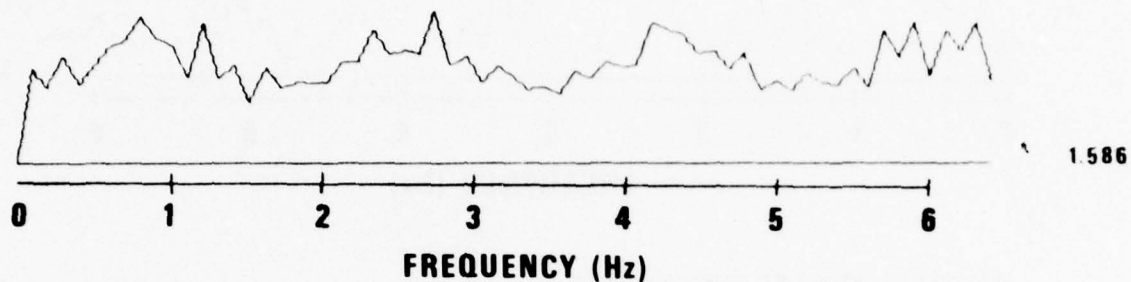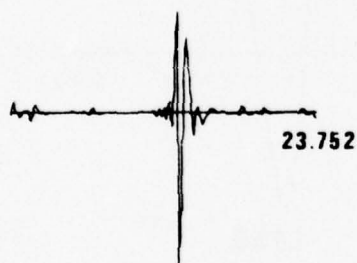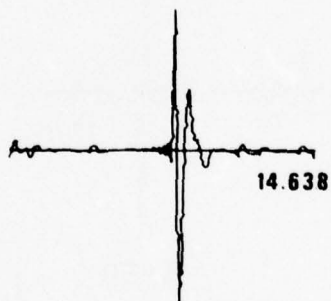
Figure 14. Crustal frequency response function, shown as linear power spectrum of the receiver crustal impulse response, receiver crust impulse responses, synthetic seismograms for the LRSM station AR-WS, NG-WS, PM-WY and RK-ON. The numbers to the right of abscissa indicate the maximum power or amplitude as appropriate.

Figure 15. Crustal frequency response function, shown as linear power spectrum of the receiver crustal impulse response, receiver crust impulse responses, synthetic seismograms for the LRSM station JE-LA. The numbers to the right of abscissa indicate the maximum power or amplitude as appropriate.
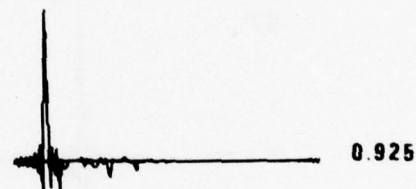
JR-AZ

CRUSTAL RESPONSE

15.500

FREQUENCY (Hz)
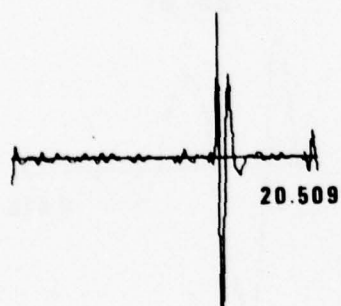
0   1   2   3   4   5   6

CRUST IMPULSE RESPONSE

SP

1.215

LP

0.771

SEISMOGRAMS

5 Kt

42.907

SP5

50 Kt

22.327

SP50

50 Kt

0.008

LP50

0   5   10

sec

0   32   64

sec
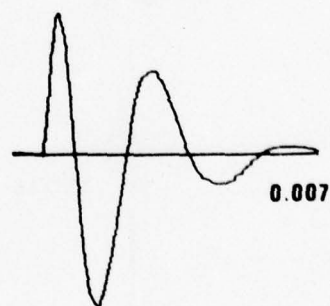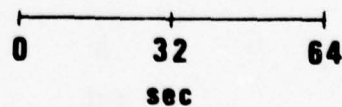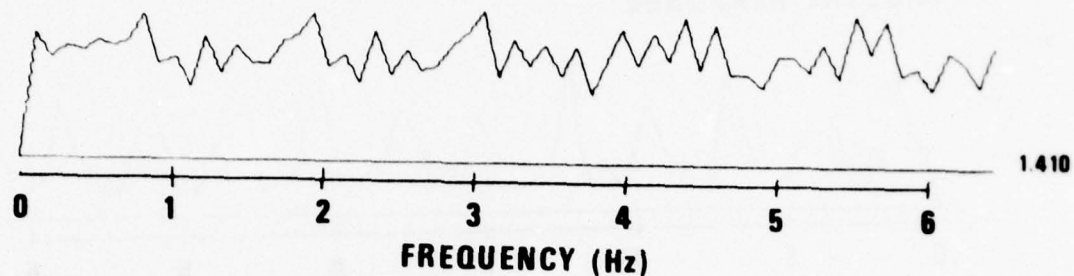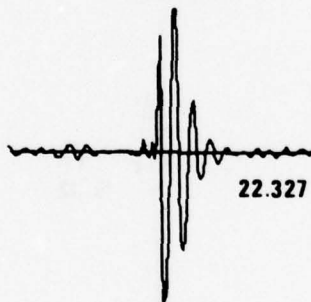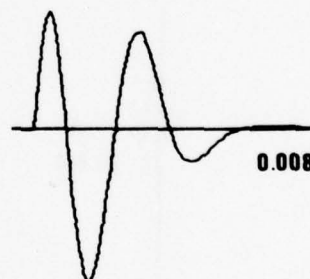
Figure 16. Crustal frequency response function, shown as linear power spectrum of the receiver crustal impulse response, receiver crust impulse responses, synthetic seismograms for the LRSM station JR-AZ. The numbers to the right of abscissa indicate the maximum power or amplitude as appropriate.

KC-MO

CRUSTAL RESPONSE

2.112

FREQUENCY (Hz)

CRUST IMPULSE RESPONSE

SP

1.039

LP

0.931

SEISMOGRAMS

5 Kt

26.810

SP5

50 Kt

15.112

SP50

50 Kt

0.007

LP50

sec

sec

Figure 17. Crustal frequency response function, shown as linear power spectrum of the receiver crustal impulse response, receiver crust impulse responses, synthetic seismograms for the LRSM station KC-MO. The numbers to the right of abscissa indicate the maximum power or amplitude as appropriate.

-36-

KN-UT

CRUSTAL RESPONSE

7.030

0   1   2   3   4   5   6
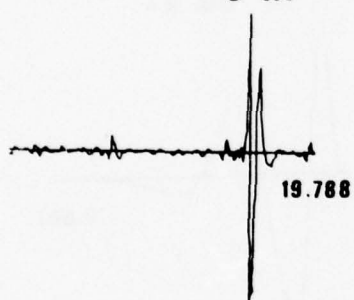
FREQUENCY (Hz)

CRUST IMPULSE RESPONSE

SP   LP

      1.396   1.259

SEISMOGRAMS

5 Kt   50 Kt   50 Kt

29.361   20.482   0.007

SP5   SP50   LP50

0   5   10   0   32   64

sec   sec

Figure 18. Crustal frequency response function, shown as linear power spectrum
of the receiver crustal impulse response, receiver crust impulse
responses, synthetic seismograms for the LRSM station KN–UT. The
numbers to the right of abscissa indicate the maximum power or
amplitude as appropriate.

-37-

LC-NM

CRUSTAL RESPONSE

FREQUENCY (Hz)

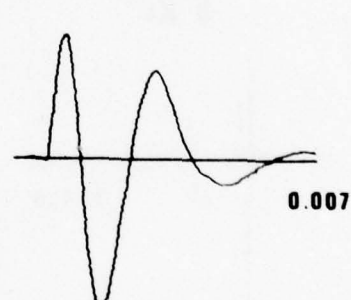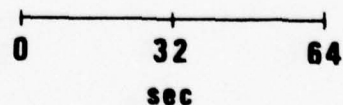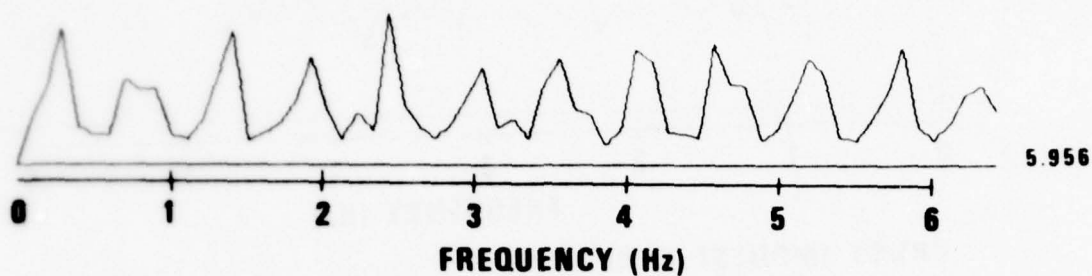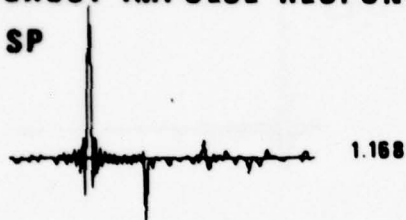**CRUST IMPULSE RESPONSE**

SP
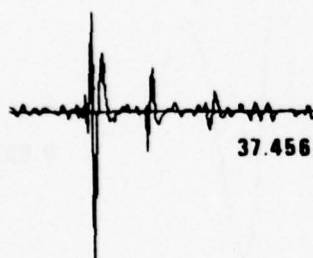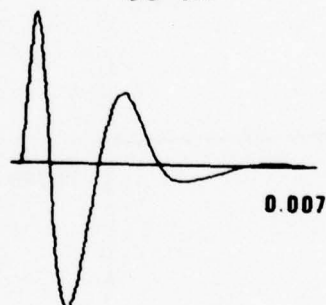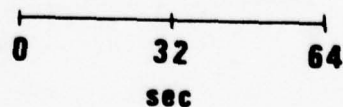
LP

SEISMOGRAMS

5 Kt

50 Kt

50 Kt

SP5

SP50

LP50

Figure 19. Crustal frequency response function, shown as linear power spectrum of the receiver crustal impulse response, receiver crust impulse responses, synthetic seismograms for the LRSM station LC-NN. The numbers to the right of abscissa indicate the maximum power or amplitude as appropriate.

LV-LA

CRUSTAL RESPONSE

8.723

FREQUENCY (Hz)

CRUST IMPULSE RESPONSE

SP

1.353

LP

1.614

SEISMOGRAMS

5 Kt

40.293

SP5

50 Kt

23.542

SP50

50 Kt

0.009

LP50

0   5   10
sec

0   32   64
sec

Figure 20.   Crustal frequency response function, shown as linear power spectrum of the receiver crustal impulse response, receiver crust impulse responses, synthetic seismograms for the LRSM station LV-LA.   The numbers to the right of abscissa indicate the maximum power or amplitude as appropriate.

MN-NV

CRUSTAL RESPONSE

1.545

FREQUENCY (Hz)

CRUST IMPULSE RESPONSE

SP   LP

0.958   0.675

SEISMOGRAMS

5 Kt   50 Kt   50 Kt

22.610   14.932   0.007

SP5   SP50   LP50

0   5   10   0   32   64
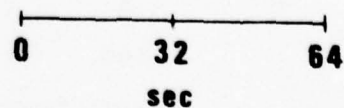
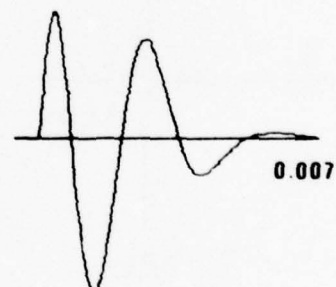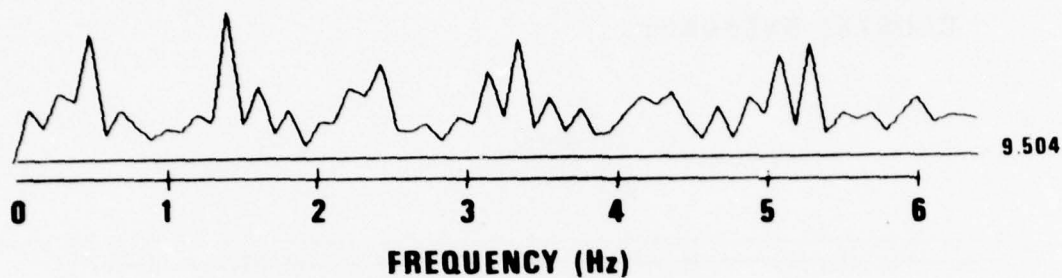sec   sec

Figure 21a. Crustal frequency response function, shown as linear power spec-
trum of the receiver crustal impulse response, receiver crust
impulse responses, synthetic seismograms for the LRSM station
MN-NV. The numbers to the right of abscissa indicate the maximum
power or amplitude as appropriate.

-40-

MO-ID

CRUSTAL RESPONSE

24.326

FREQUENCY (Hz)

CRUST IMPULSE RESPONSE

SP

LP

1.674

1.921

SEISMOGRAMS

5 Kt

50 Kt

50 Kt

44.682

27.905

0.007

SP5
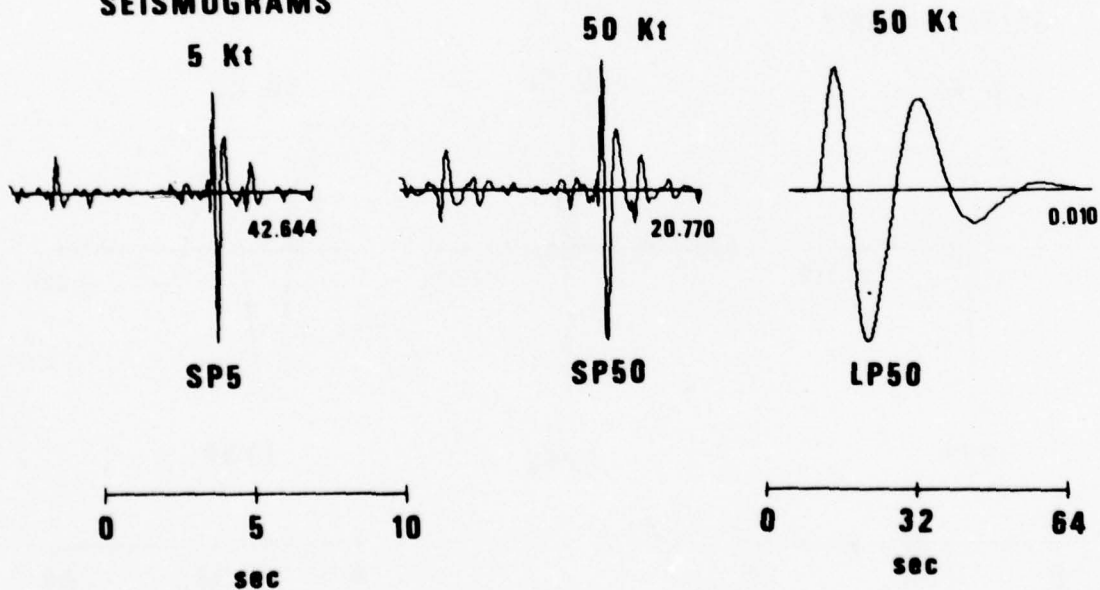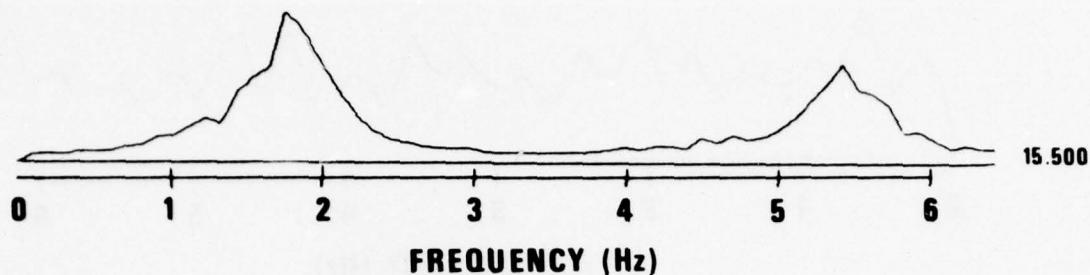
SP50

LP50

0   5   10

sec

0   32   64

sec

Figure 21b.   Crustal frequency response function, shown as linear power spec-
trum of the receiver crustal impulse response, receiver crust
impulse responses, synthetic seismograms for the LRSM station
MO-ID.   The numbers to the right of abscissa indicate the maximum
power or amplitude as appropriate.

MV-CL

CRUSTAL RESPONSE

FREQUENCY (Hz)

CRUST IMPULSE RESPONSE

SP   LP

SEISMOGRAMS

5 Kt   50 Kt   50 Kt

SP5   SP50   LP50

Figure 22. Crustal frequency response function, shown as linear power spectrum
of the receiver crustal impulse response, receiver crust impulse
responses, synthetic seismograms for the LRSM station MV-CL. The
numbers to the right of abscissa indicate the maximum power or
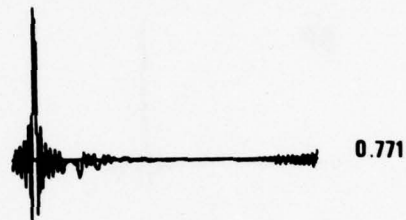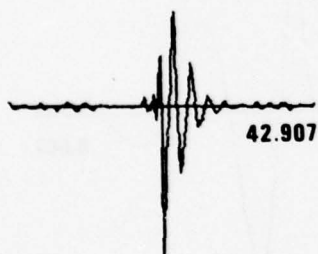amplitude as appropriate.

NP-NT

CRUSTAL RESPONSE

3.571

FREQUENCY (Hz)

CRUST IMPULSE RESPONSE

SP

1.178

LP

1.109

SEISMOGRAMS

5 Kt

29.266

SP5

50 Kt

17.125

SP50

50 Kt

0.007

LP50

sec

sec

Figure 23. Crustal frequency response function, shown as linear power spectrum of the receiver crustal impulse response, receiver crust impulse responses, synthetic seismograms for the LRSM station NP-NT. The numbers to the right of abscissa indicate the maximum power or amplitude as appropriate.

-43-

PG-BC

CRUSTAL RESPONSE

FREQUENCY (Hz)

CRUST IMPULSE RESPONSE

SP   LP

0.988   1.092
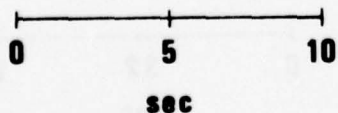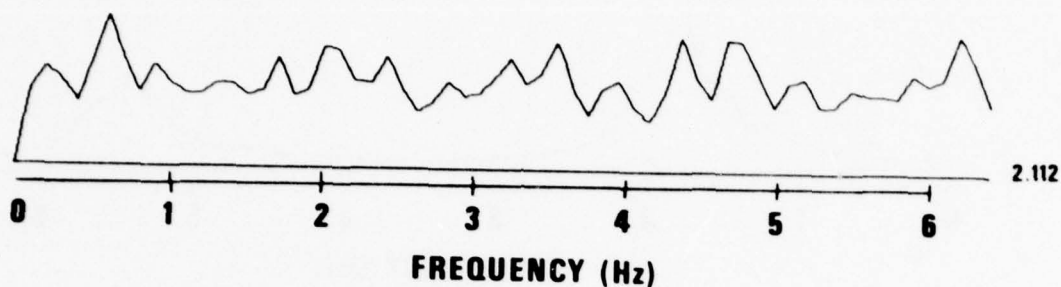
SEISMOGRAMS

5 Kt   50 Kt   50 Kt

25.238   15.760   0.008

SP5   SP50   LP50

0   5   10   0   32   64
         sec   sec
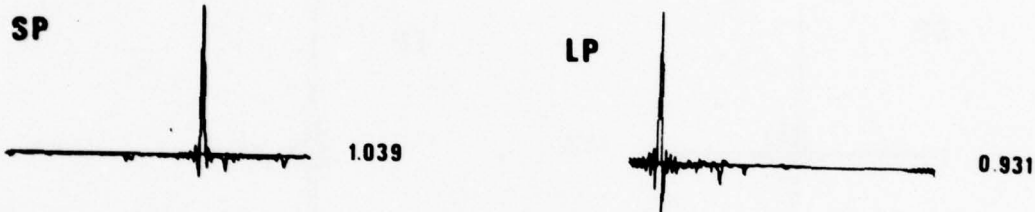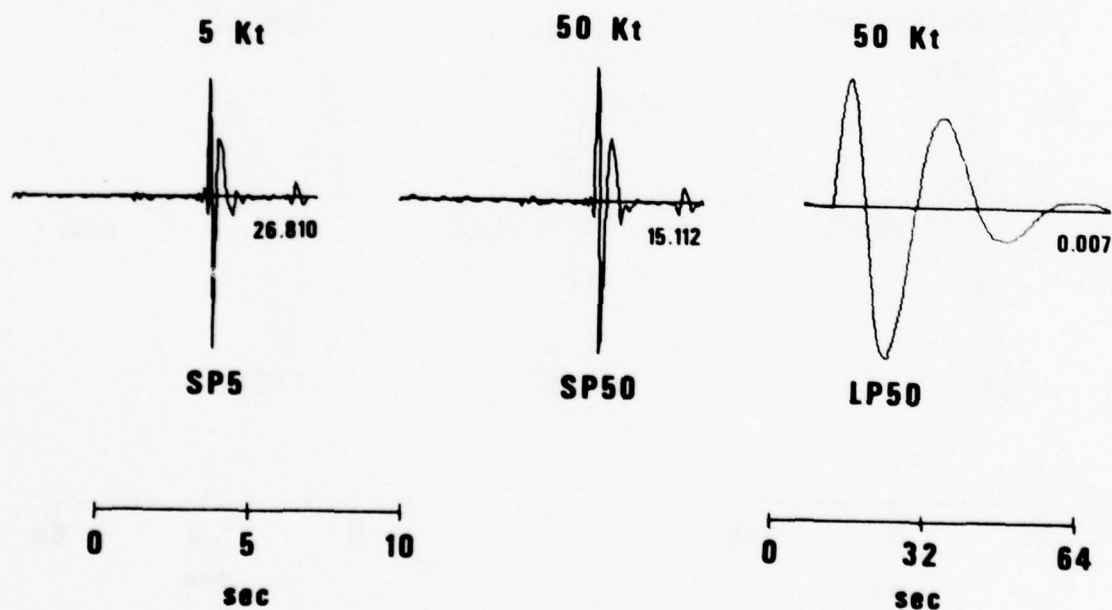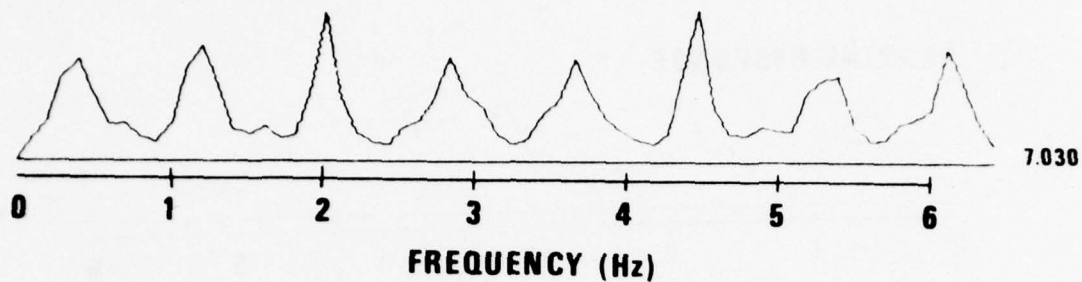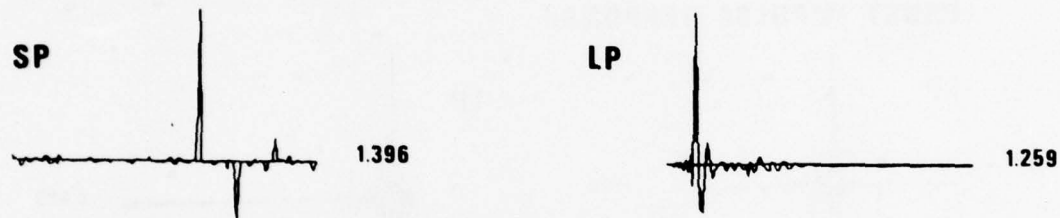
Figure 24.   Crustal frequency response function, shown as linear power spectrum
             of the receiver crustal impulse response, receiver crust impulse
             responses, synthetic seismograms for the LRSM station PG-BC. The
             numbers to the right of abscissa indicate the maximum power or
             amplitude as appropriate.

SJ-TX

CRUSTAL RESPONSE

14.959

FREQUENCY (Hz)

CRUST IMPULSE RESPONSE

SP   **LP**

1.684   1.344

SEISMOGRAMS

5 Kt   **50 Kt**   **50 Kt**

45.287   26.899   0.011

SP5   **SP50**   **LP50**

0   5   10   0   32   64

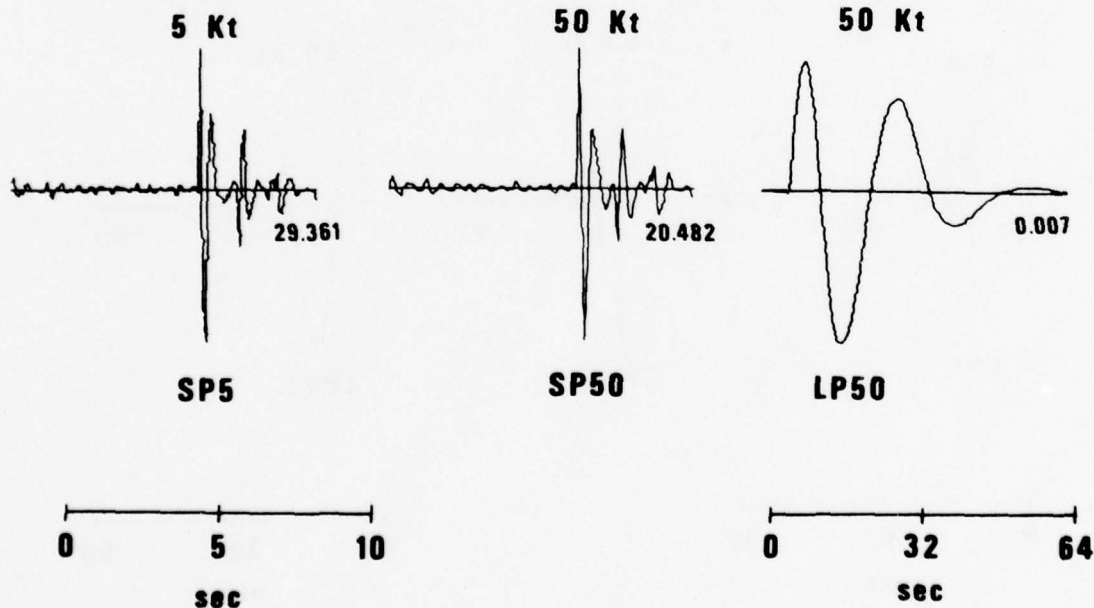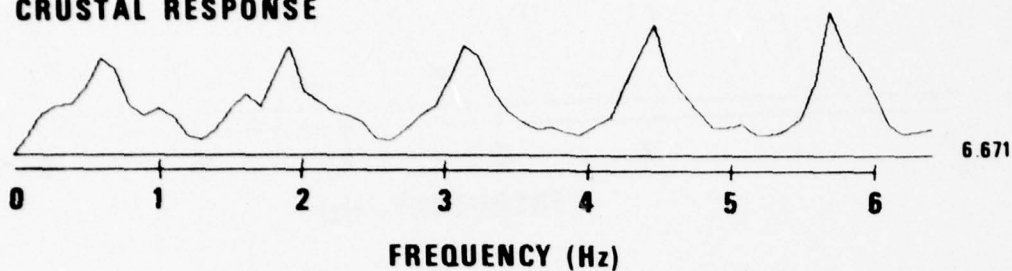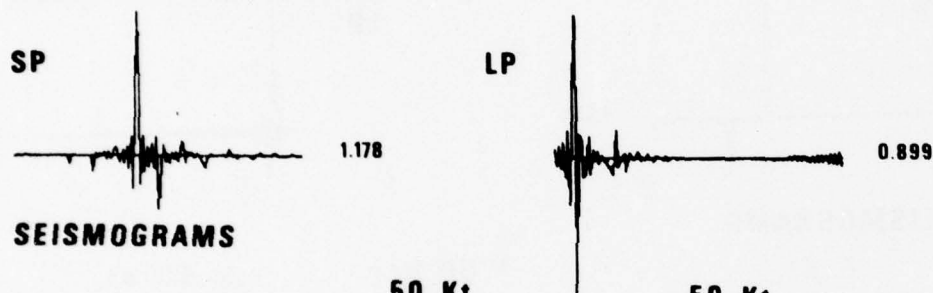sec   sec
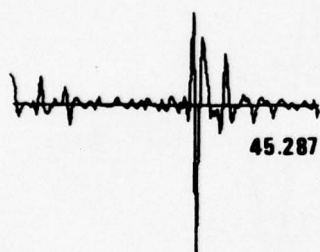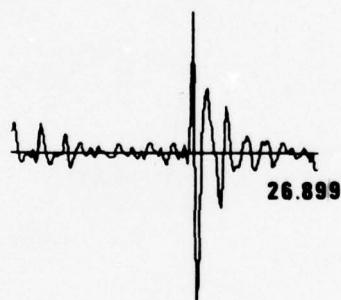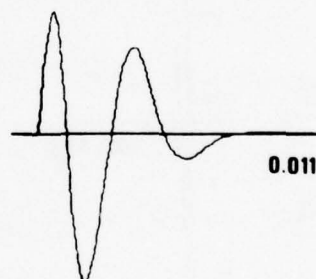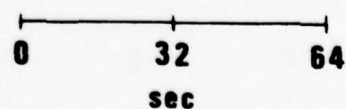
Figure 25.   Crustal frequency response function, shown as linear power spectrum
of the receiver crustal impulse response, receiver crust impulse
responses, synthetic seismograms for the LRSM station SJ-TX.   The
numbers to the right of abscissa indicate the maximum power or
amplitude as appropriate.

-45-

SV-QB

CRUSTAL RESPONSE

1.571

0 1 2 3 4 5 6

FREQUENCY (Hz)

CRUST IMPULSE RESPONSE

SP

1.002

LP

0.973

SEISMOGRAMS

5 Kt

20.496

50 Kt

14.851

50 Kt

0.007

SP5

SP50

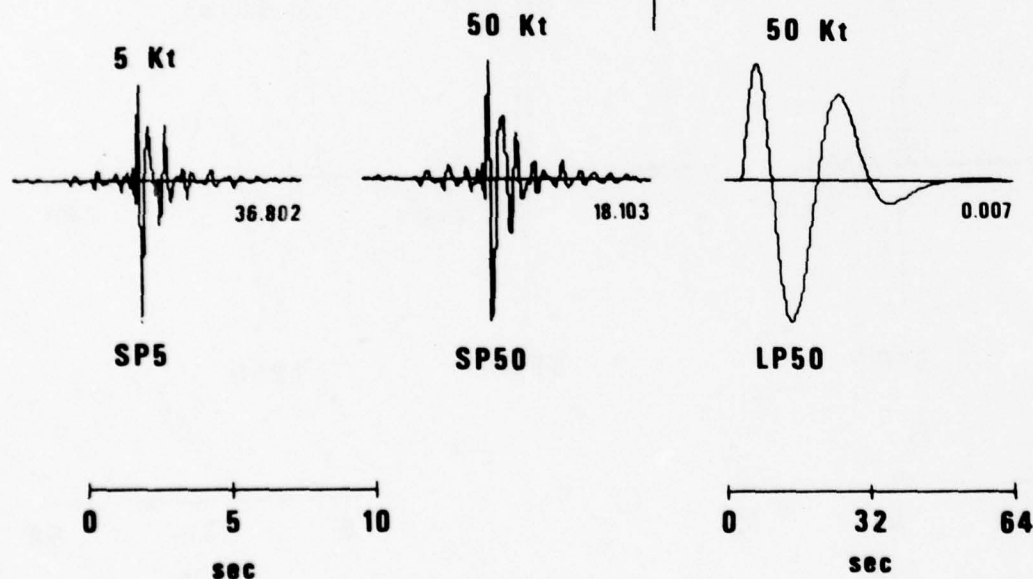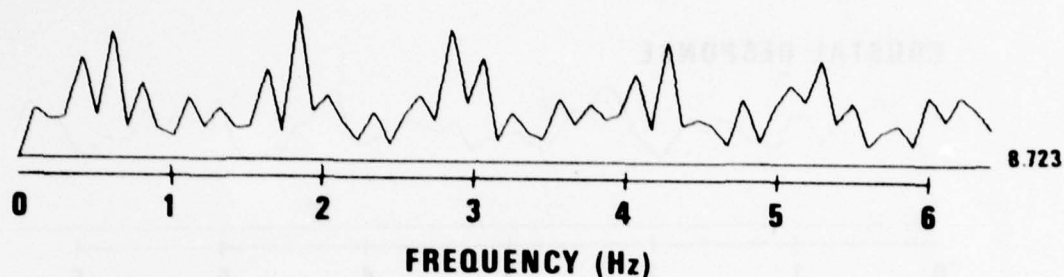LP50

0   5   10
sec

0   32   64
sec
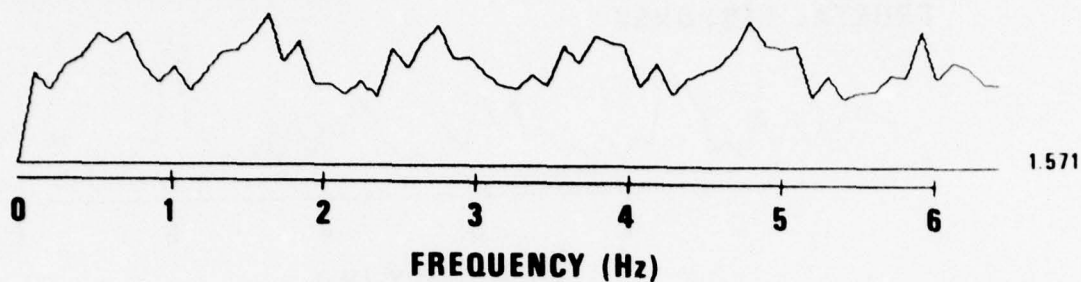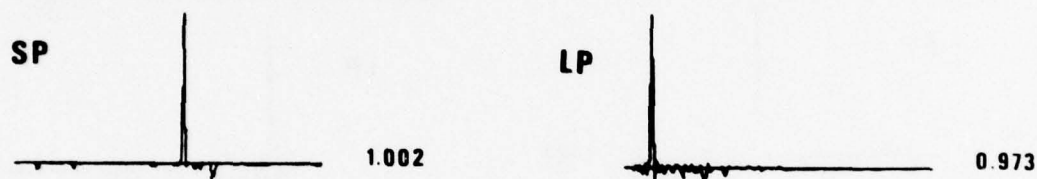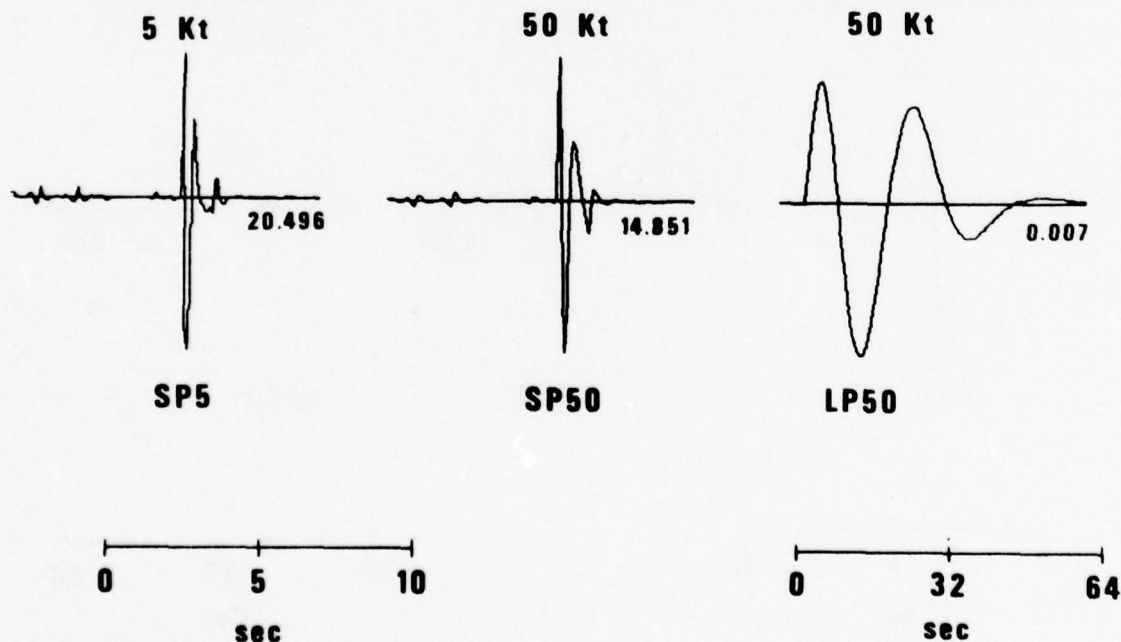
Figure 26. Crustal frequency response function, shown as linear power spectrum of the receiver crustal impulse response, receiver crust impulse responses, synthetic seismograms for the LRSM station SV-QB. The numbers to the right of abscissa indicate the maximum power or amplitude as appropriate.

SW-MA

CRUSTAL RESPONSE

1.970

FREQUENCY (Hz)

CRUST IMPULSE RESPONSE

SP   LP

0.942   0.888

SEISMOGRAMS

5 Kt   50 Kt   50 Kt

27.814   16.171   0.007

SP5   SP50   LP50

0   5   10   0   32   64

sec   sec
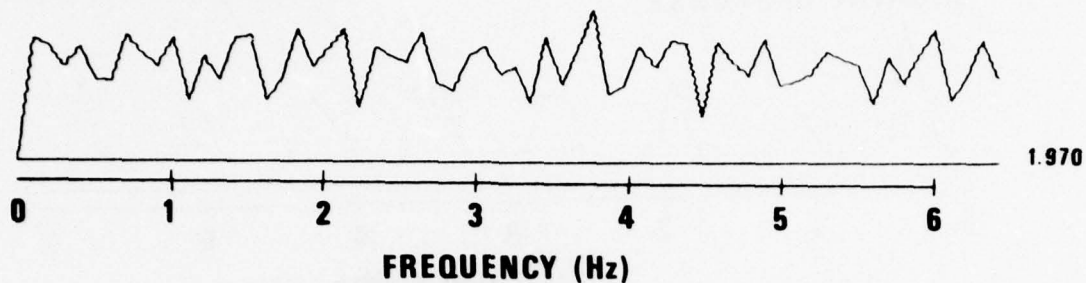
Figure 27. Crustal frequency response function, shown as linear power spectrum
of the receiver crustal impulse response, receiver crust impulse
responses, synthetic seismograms for the LRSM station SW-MA. The
numbers to the right of abscissa indicate the maximum power or
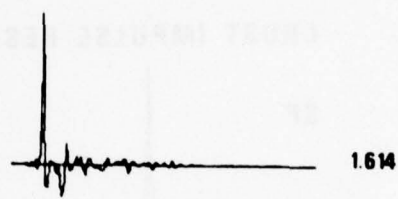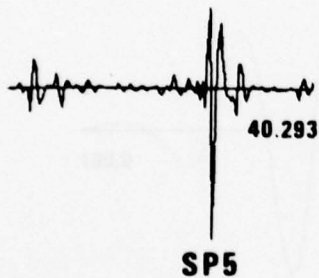amplitude as appropriate.

-47-

TF-CL

CRUSTAL RESPONSE

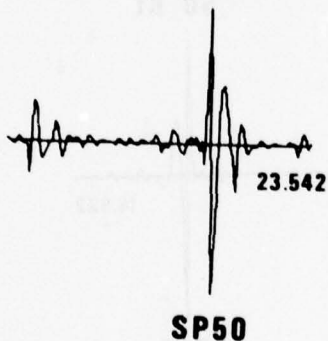9.383

FREQUENCY (Hz)

CRUST IMPULSE RESPONSE

SP   1.248   LP   1.104

SEISMOGRAMS

5 Kt   50 Kt   50 Kt

34.167   20.359   0.008

SP5   SP50   LP50

0   5   10   0   32   64
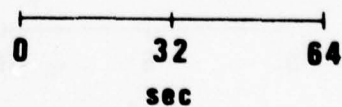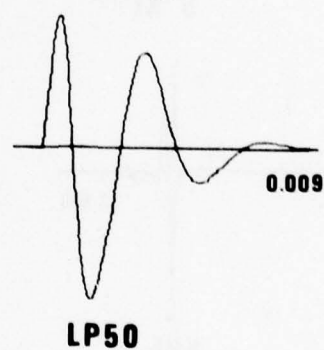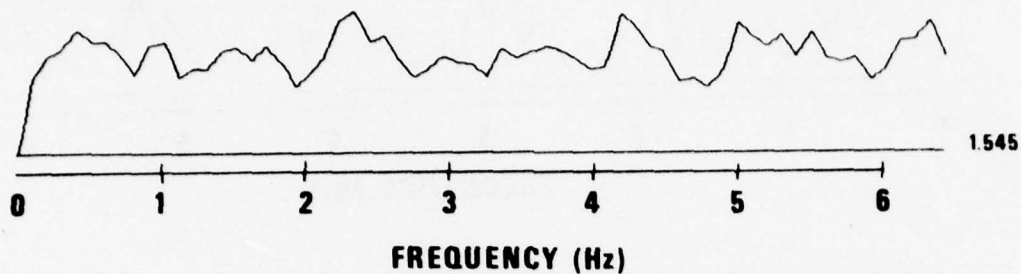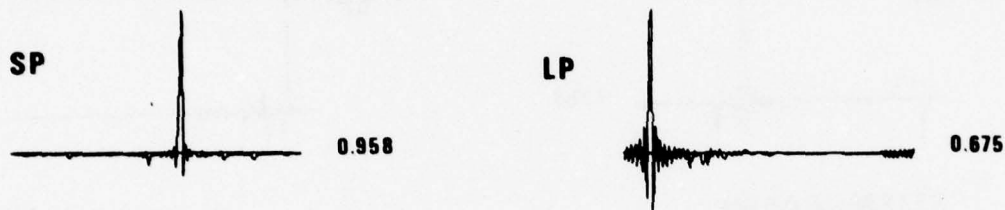
sec   sec
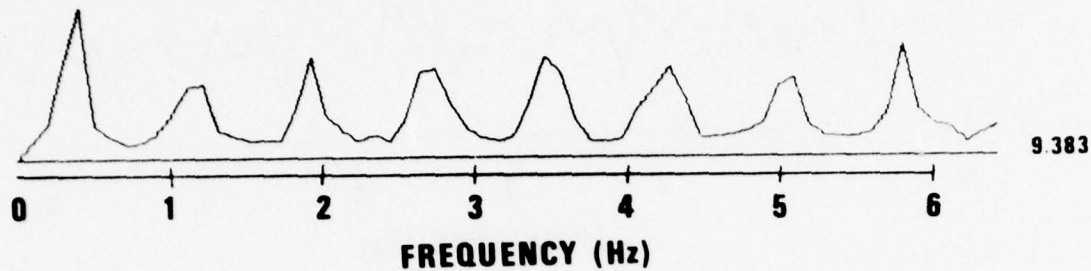
Figure 28. Crustal frequency response function, shown as linear power spectrum
of the receiver crustal impulse response, receiver crust impulse
responses, synthetic seismograms for the LRSM station TF-CL. The
numbers to the right of abscissa indicate the maximum power or
amplitude as appropriate.

-48-

WH-YK

CRUSTAL RESPONSE

1.443

FREQUENCY (Hz)

CRUST IMPULSE RESPONSE

SP

0.638

LP

0.807

SEISMOGRAMS

5 Kt

25.950

SP5

50 Kt
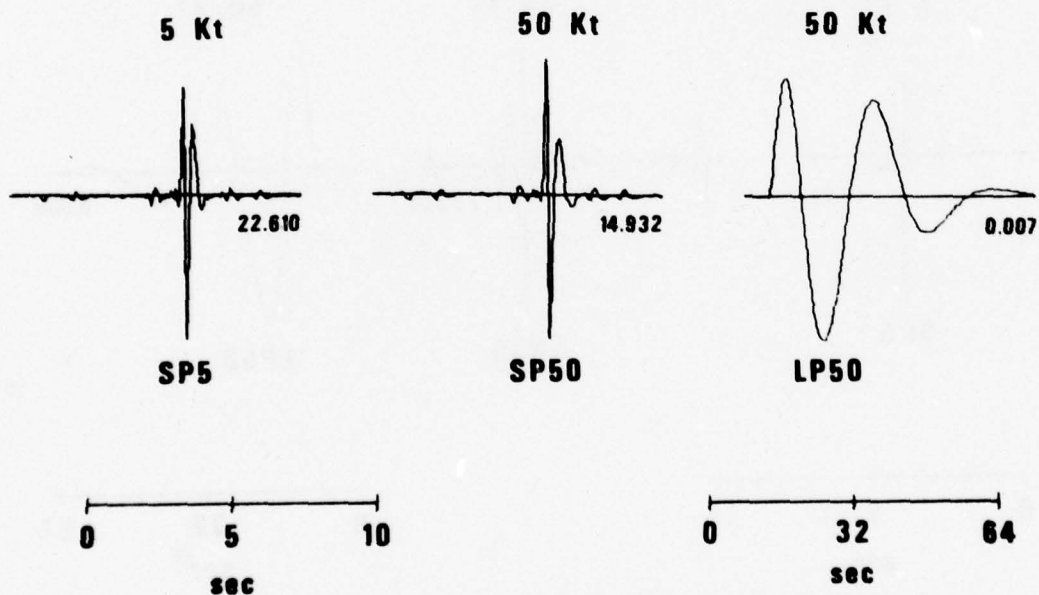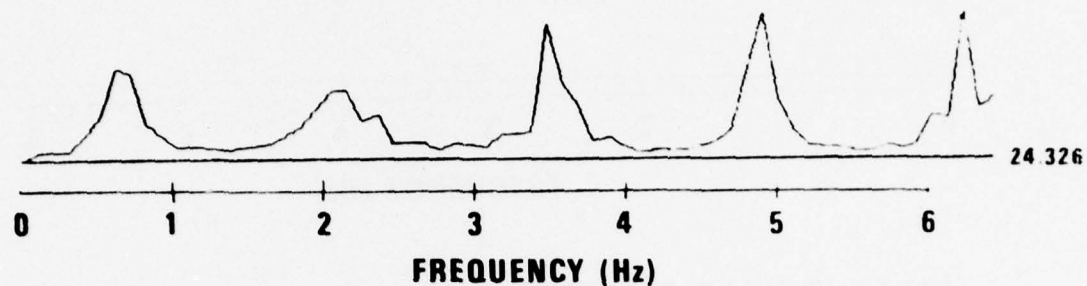

13.156

SP50

50 Kt

0.007

LP50

sec

sec
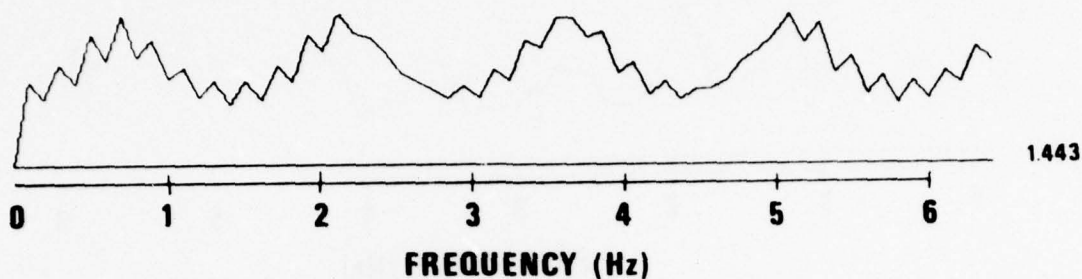
Figure 29. Crustal frequency response function, shown as linear power spectrum
of the receiver crustal impulse response, receiver crust impulse
responses, synthetic seismograms for the LRSM station WH-YK. The
numbers to the right of abscissa indicate the maximum power or
amplitude as appropriate.

WI-NV

CRUSTAL RESPONSE

CRUST IMPULSE RESPONSE

SP   1.158   LP   0.982

SEISMOGRAMS

5 Kt   50 Kt   50 Kt
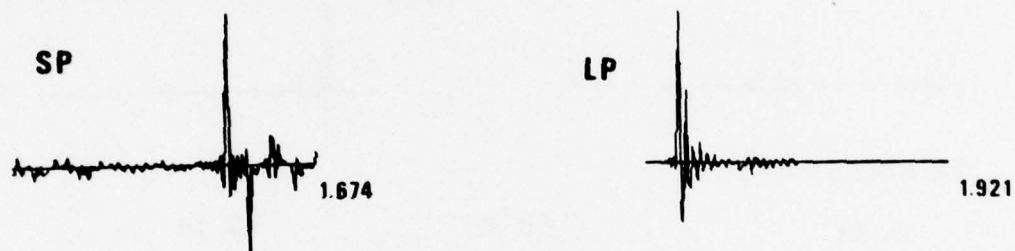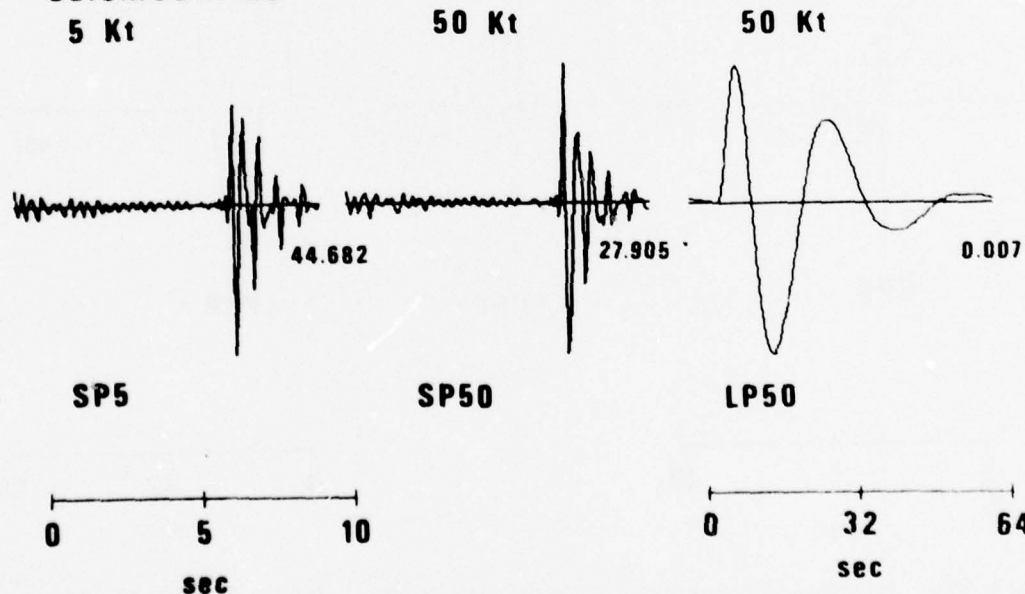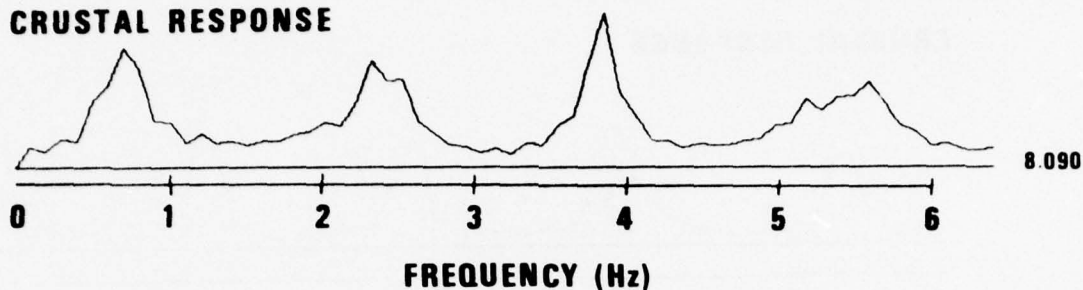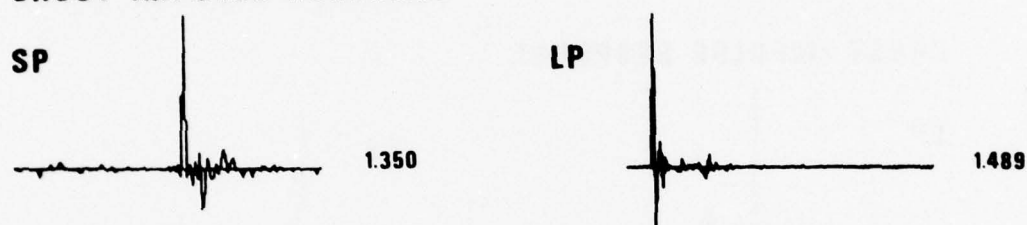
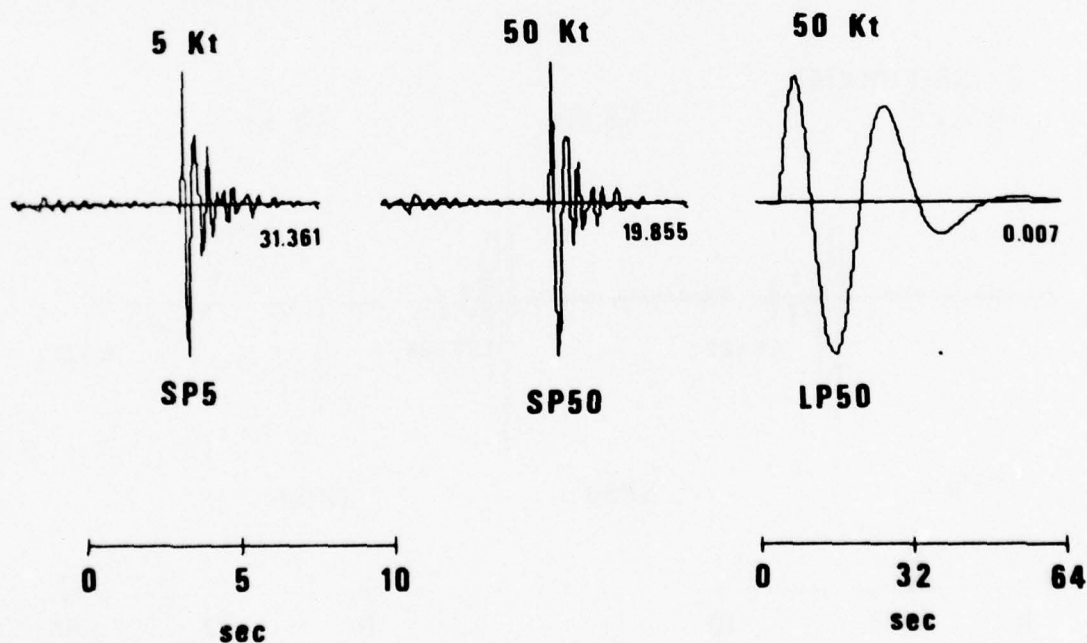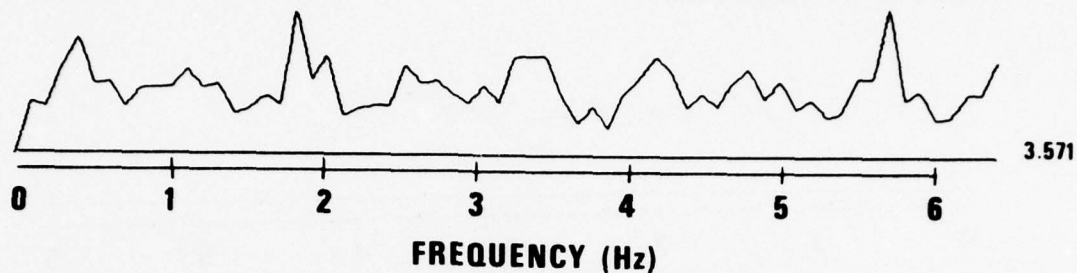26.301   17.150   0.008

SP5   SP50   LP50
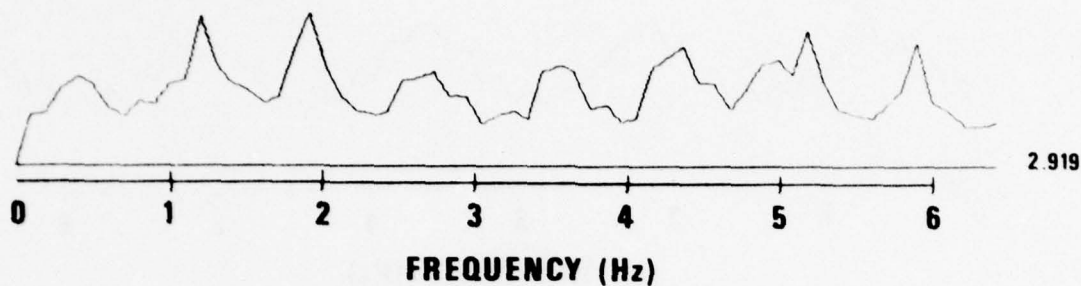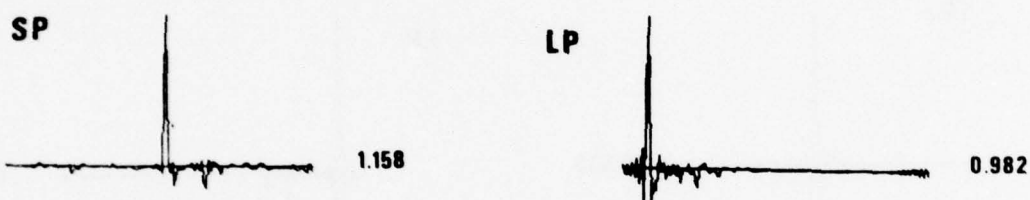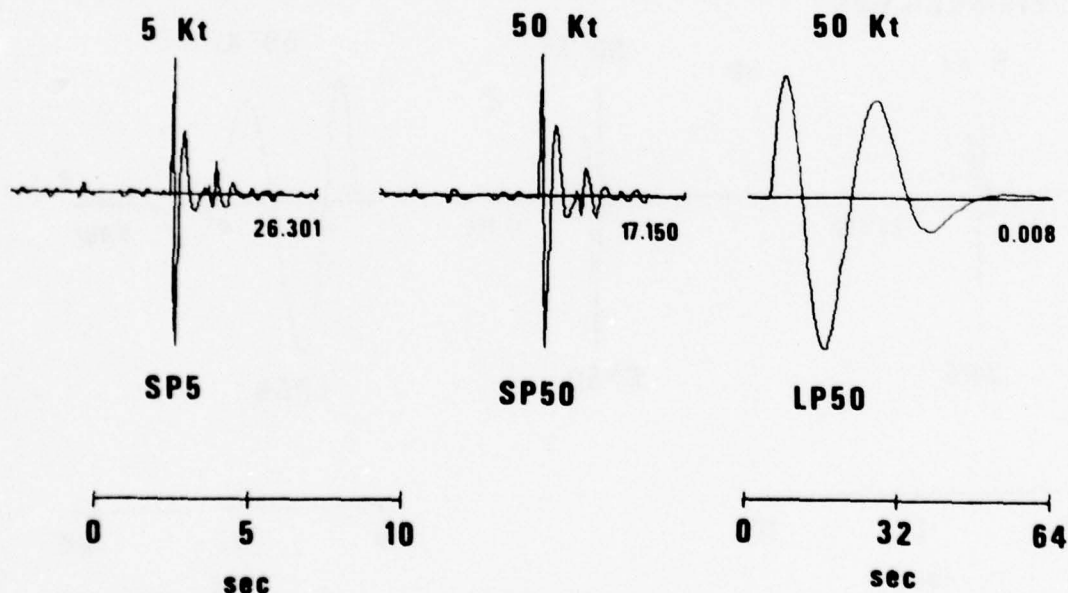
Figure 30. Crustal frequency response function, shown as linear power spectrum of the receiver crustal impulse response, receiver crust impulse responses, synthetic seismograms for the LRSM station WI-NV. The numbers to the right of abscissa indicate the maximum power or amplitude as appropriate.
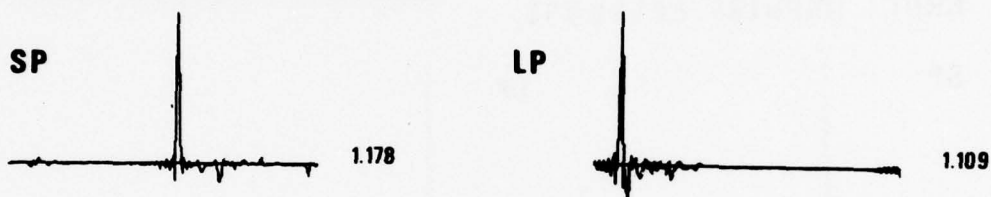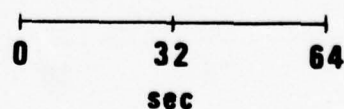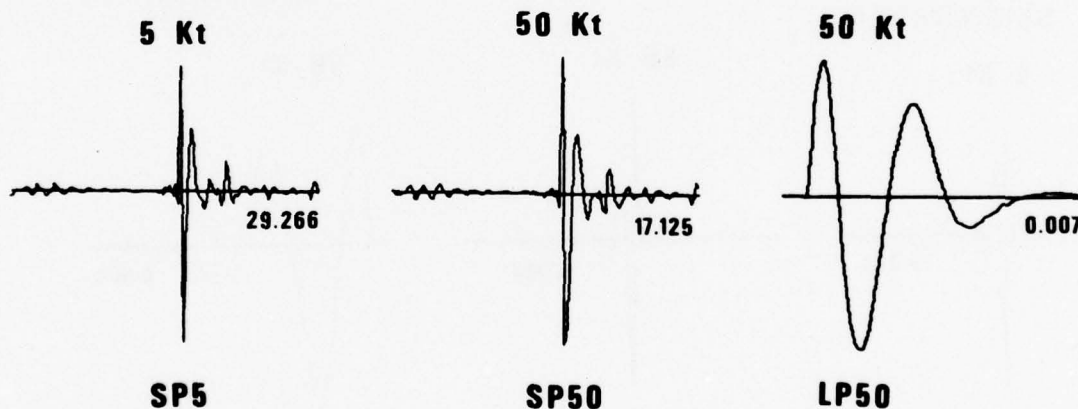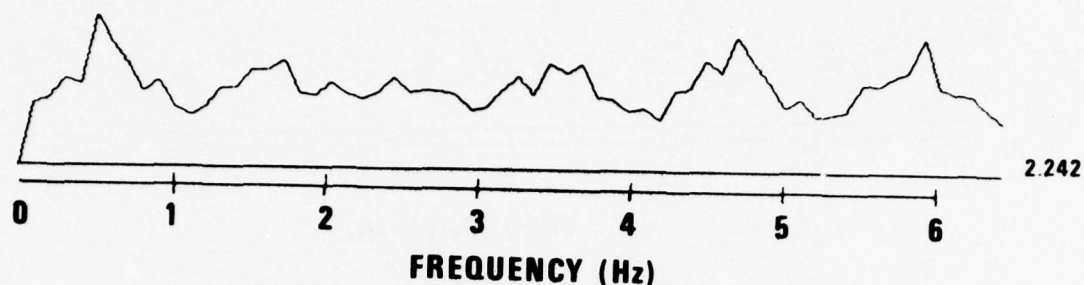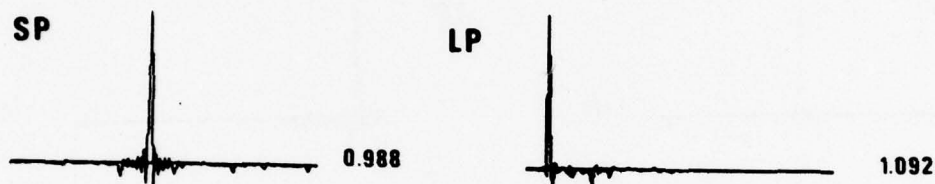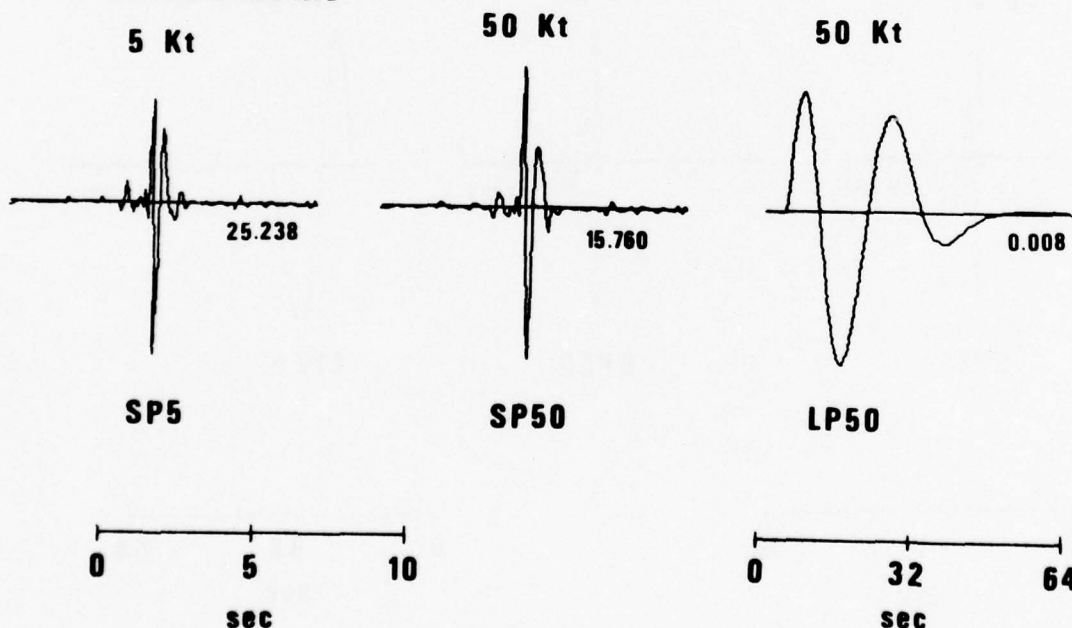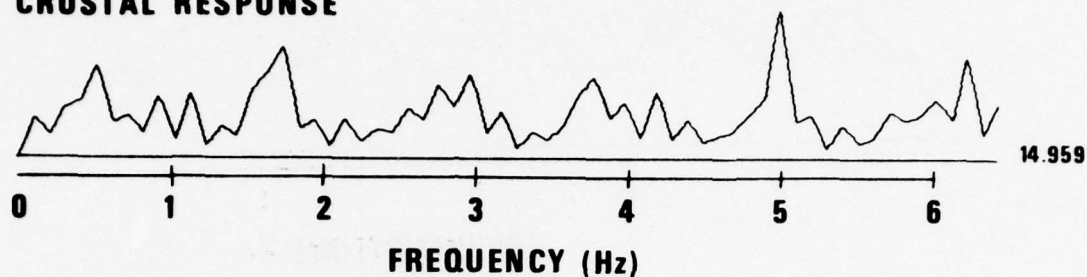
The results of calculations show that the total variation in magnitude due to the estimated plane-parallel crustal structure is much less than the observed variation in magnitude residuals. The largest values of crustal amplification are associated with thick sediments at the surface, at Gulf Coast stations LVLA and SJTX for example. Since these models are some extreme it is unlikely that credible refinements in the crustal structures would increase the range of crustal amplification. Major modifications of structures can, in most cases, be ruled out even on the basis of the sketchy geological information available.

For instance, although addition of thin (d < 100m), low-velocity weathered layer or a thin layer of alluvium could be allowed at some sites by the available geological information, it would be unlikely to introduce any significant change in the results. Similarly, it would be unreasonable to assume low velocities for sedimentary rocks at some EUS stations, if it is stated in the site description that these rocks are highly compact or metamorphized. If a station located on granite bedrock the obvious choice is to use a simple two layer crust with a granitic top layer. This would be incorrect only if the dimensions of the granite body are extremely small. The thicknesses conform everywhere with the regional crustal thicknesses given by Pakiser and Steinhart (1964), and with the nearby crustal refraction studies and the P_n velocities given by Herrin and Taggart (1962).

Tables IIa and IIb summarize the results of our calculations. Table IIa indicates the areal subdivision used (1 for EUS, 2 for WUS, 3 for others), gives values of density and P wave velocity at the surface (α_s, ρ_s) and below the Moho (α_n, ρ_n) and the raw vertical surface amplitudes obtained by the Haskell matrix method for the 5 kt and 50 kt pulses as viewed through the LRSM short and long period instruments ($\overline{SP5}$, $\overline{SP50}$, $\overline{LP50}$). These include various common factors in the computations due to pulse shape, Fourier transforms etc. which are of no interest since only the relative pulse amplitude ratios between

Pakiser, L. C., and J. S. Steinhart (1964). Explosion seismology in the Western Hemisphere, Research in Geophysics, 2, MIT Press.

Herrin, E. T., and J. Taggart (1962). Regional variations in P_n velocity and their effect on the location of epicenter, Bull. Seism. Soc. Am., 52, 1037-1046.

TABLE IIa

Table of surface and sub-Moho material constants, raw readings from synthetic seismograms, and magnitude residuals of Booth et al. (1974).

STATION	Regional subdivisions	α_s	ρs	α_n	ρ_n	$\overline{SP5}$	$\overline{SP50}$	$\overline{LP50}$	SPC	LPC
ADIS	3	5.50	2.70	8.10	3.30	20.411	15.009	0.00749	0.33	0.09
ARWS	1	5.64	2.70	8.10	3.30	23.752	14.638	0.00716	-0.04	-0.14
AXAI	1	6.00	2.70	8.10	3.30	24.160	14.105	0.00721	0.10	0.10
BETI	1	2.60	1.80	8.10	3.30	43.714	22.053	0.00742	0.33	0.35
BLWV	1	5.00	2.70	8.14	3.53	23.103	14.734	0.00738	0.08	-0.01
BFPA	1	6.00	2.70	8.14	3.53	23.103	14.734	0.00738	0.02	0.47
CPCI	2	5.82	2.60	7.90	3.30	25.479	13.668	0.00755	-0.35	-0.04
DHNY	1	6.00	2.70	8.14	3.53	23.103	14.734	0.00738	0.10	0.01
DRCO	2	6.00	2.70	7.80	3.30	20.843	14.129	0.00589	-0.25	-0.11
FKCO	1	2.90	1.80	8.00	3.30	34.551	22.761	0.00739	0.19	0.29
FMUT	2	3.40	2.30	7.40	3.10	23.567	18.138	0.00727	-0.14	-0.19
GVTX	1	3.05	1.80	8.20	3.40	45.344	21.034	0.00760	0.30	0.04
HLID	2	5.20	2.50	7.90	3.20	20.500	15.421	0.00681	-0.16	-0.14
HNME	1	5.90	2.70	8.10	3.30	19.788	14.562	0.00739	0.08	-0.09
HWIS	3	3.70	1.94	8.20	3.40	37.456	18.108	0.00685	0.27	-0.06
JELA	1	2.70	2.00	8.10	3.30	42.644	20.770	0.01010	0.28	0.26
JRAZ	2	2.50	1.80	7.90	3.30	42.907	22.327	0.00769	-0.16	-0.05
KCMO	1	5.00	2.60	8.09	3.30	26.810	15.112	0.00719	-0.12	-0.13
KNUT	2	3.15	2.00	7.80	3.20	29.361	20.482	0.00702	-0.04	-0.03
LCNM	2	3.00	2.20	7.90	3.30	36.802	18.103	0.00722	-0.22	-0.19
LVIA	1	2.70	2.00	8.10	3.30	40.293	23.542	0.00929	0.19	0.04
MNNV	2	5.80	2.50	7.80	3.30	22.610	14.932	0.00715	-0.28	-0.09
MOID	2	1.50	1.80	7.90	3.20	44.682	27.606	0.00681	0.41	-0.37
MVCI	2	3.00	2.20	7.80	3.30	31.361	19.855	0.00726	-0.32	-0.10
NGWS	1	5.64	2.70	8.10	3.30	23.752	14.638	0.00716	-0.02	-0.08
NPNT	1	4.33	2.40	8.20	3.30	29.266	17.125	0.00696	0.19	0.13
PGBC	2	5.00	2.60	8.00	3.30	25.256	15.760	0.00759	-0.12	-0.03
PMWY	2	5.64	2.70	8.10	3.30	23.752	14.638	0.00716	-0.23	-0.07
RKON	1	5.64	2.70	8.10	3.30	23.752	14.638	0.00716	0.07	-0.06
SJTX	1	2.13	1.80	8.00	3.30	45.287	26.899	0.01080	0.17	-0.09
SVOB	1	5.80	2.60	8.00	3.30	20.496	14.851	0.00732	0.19	0.03
SWMA	1	5.00	2.50	8.00	3.30	27.814	16.171	0.00722	0.04	-0.23
TECI	2	3.00	2.00	8.10	3.30	24.165	20.359	0.00786	-0.24	0.04
WHVK	3	6.20	2.75	8.20	3.30	25.960	13.156	0.00717	-0.07	-0.10
WINV	2	4.50	2.30	7.90	3.20	26.301	17.150	0.00762	-0.28	-0.10

TABLE IIb

Table of crustal amplification terms, surface impedance terms and magnitude residuals of Booth et al. (1974).

STATION	Regional subdivision	Crustal amplification terms			Surface impedance term $\log_{10}\sqrt{\rho\alpha_s^3}$	Short period magnitude residuals Δm_b SP	Long period magnitude residuals
		5kt pulse SP	50kt pulse SP	LP		Booth et al, 1974	
ADIS	3	1.?8	1.15	0.84	1.?3	0.?3	0.08
ARWS	1	1.34	1.13	0.82	1.?4	-0.04	-0.14
AXAI	1	1.35	1.12	0.8?	1.?8	0.10	0.19
BEEL	1	1.61	1.31	0.84	0.75	0.33	0.35
BLWV	1	1.31	1.12	0.82	1.38	0.08	-0.01
BRPA	1	1.31	1.12	0.82	1.38	-0.02	0.47
CPCI	2	1.30	1.12	0.86	1.35	-0.02	-0.04
DHNY	1	1.31	1.12	0.82	1.38	0.10	0.01
DRCO	2	1.31	1.14	0.83	1.38	-0.25	-0.11
EKCO	1	1.52	1.33	0.95	0.82	0.10	0.28
FMUT	2	1.41	1.30	0.90	0.88	-0.15	-0.10
GVTX	1	1.61	1.30	0.84	0.85	0.30	0.04
HLID	2	1.30	1.18	0.82	1.27	-0.16	-0.14
HNME	1	1.27	1.13	0.84	1.37	0.08	-0.09
HWIS	3	1.53	1.21	0.79	1.00	0.27	-0.06
JELA	1	1.60	1.29	0.97	0.80	0.28	0.26
JRAZ	2	1.62	1.33	0.87	0.72	-0.16	-0.05
KCMO	1	1.40	1.15	0.83	1.26	0.12	-0.13
KNUT	2	1.47	1.31	0.85	0.90	-0.04	0.03
LCNM	2	1.55	1.24	0.84	0.89	-0.22	-0.19
LVIA	1	1.57	1.34	0.94	0.80	-0.16	0.04
MNNV	2	1.35	1.17	0.85	1.34	-0.28	0.00
MOID	2	1.64	1.44	0.92	0.30	0.41	-0.37
MVCL	2	1.49	1.29	0.85	0.89	-0.32	-0.10
NGWS	1	1.34	1.13	0.82	1.34	-0.02	-0.08
NPNT	1	1.43	1.19	0.80	1.14	0.19	0.13
PGBC	2	1.38	1.17	0.86	1.26	-0.12	-0.03
PMWY	2	1.34	1.13	0.82	1.34	-0.23	-0.07
RKON	1	1.34	1.13	0.82	1.34	0.07	-0.06
SJTX	1	1.63	1.41	1.01	0.62	0.17	-0.09
SVQB	1	1.29	1.15	0.84	1.35	0.19	-0.03
SWMA	1	1.42	1.10	0.84	1.25	0.04	-0.23
TFCI	2	1.50	1.28	0.86	0.87	-0.24	0.04
WHYK	3	1.38	1.08	0.82	1.41	-0.07	-0.10
WINV	2	1.41	1.23	0.87	1.16	-0.28	-0.10

various stations matter. The magnitude residuals of Booth et al. (1964) for short and long period P waves (SPC and LPC) are also given. Table IIb shows reduced quantities to be analyzed. We correct for the sub-Moho medium by dividing the calculated amplitudes by $\sqrt{\rho_n \alpha_n^3}$. We denote the quantities thus corrected by the unbarred designations SP5, SP50, LP50. The base ten logarithms of these are named <u>crustal amplification terms</u> in this report. We name the quantity $\log_{10}(\sqrt{\rho_s \alpha_s^3})$ the surface impedance term. To examine the question of whether a difference in observed magnitude is proportional to a difference in the logarithm of theoretical amplitudes, the absolute level of the individuals comprising the pair of theoretical amplitudes is irrelevant. We are, therefore, free to subtract a constant from the logarithms of the amplitudes of, e.g., $\overline{SP5}$ in Table IIa. A different constant has been subtracted from the logs of each of the columns SP5, SP50, and LP50, after they have been corrected for $\sqrt{\rho_n \alpha_n^3}$, in order to bring the numbers into the range of unity. The last two columns of Table IIa contain the magnitude correction terms given by Booth, Marshall and Young (1974) for short and long period P-waves. [Since in the following regression analysis we want to test the dependence of the magnitude correction on crustal structure together with t*; in accordance with Der et al. (1977), we choose t* = 0.2 for EUS stations and t* = .45 for WUS stations. These averages are broadly valid; no reliable t* figures are available for individual stations at this writing. Individual station t* values could be obtained by averaging many individual spectral observations at each station, and it seems certain that they would reduce the final error variance.]

In preparing for the regression analysis let us first examine visually some plots of our computed crustal amplification terms vs. other relevant quantities. We show in Figures 31 and 32 the short period amplification terms from Table IIb (log-amplitude) plotted against the quantity $\log_{10}(\sqrt{\rho_s \alpha_s^3})$, where the subscripts s pertain to estimated vales of ρ and α at the free surface. The figures show that the surface properties are very important in

Der, Z. A., M. S. Dawkins, T. W. McElfresh, J. H. Goncz, C. E. Gray, M. S. Gillispie (1977). Teleseismic P Wave Amplitudes and Spectra at NTS and the Shoal Site as Compared to Those Observed in Eastern North America, Preliminary Report, SDAC-TR-77-9, Teledyne Geotech, Alexandria, Va.

$$\log_{10}(SP50) = -.327 \log_{10} \left(\sqrt{\rho_s \, \alpha_s^3} \right) + CONST$$

LEGEND
△ WUS
□ EUS
○ OTHER

SURFACE IMPEDANCE TERMS $\left[\log_{10} \left(\sqrt{\rho_s \, \alpha_s^3} \right) \right]$

COMPUTED SHORT PERIOD CRUSTAL AMPLIFICATION TERM ($\log_{10}$ SP50) 50 kt PULSE

Figure 31. Short period crustal amplification term for a pulse from a 50 kt nuclear explosion plotted against the surface acoustic impedance term. Least squares regression line is drawn through the points.

COMPUTED SHORT PERIOD CRUSTAL AMPLIFICATION TERMS ($\log_{10}$ SP5) 5 kt PULSE

SURFACE IMPEDANCE TERMS [$\log_{10} (\sqrt{\rho_s \, \alpha_s^3})$]

$\log_{10}(SP5) = -.393 \log_{10} \sqrt{\rho_s \, \alpha_s^3} + CONST$

LEGEND
△ WUS
○ EUS
□ OTHER
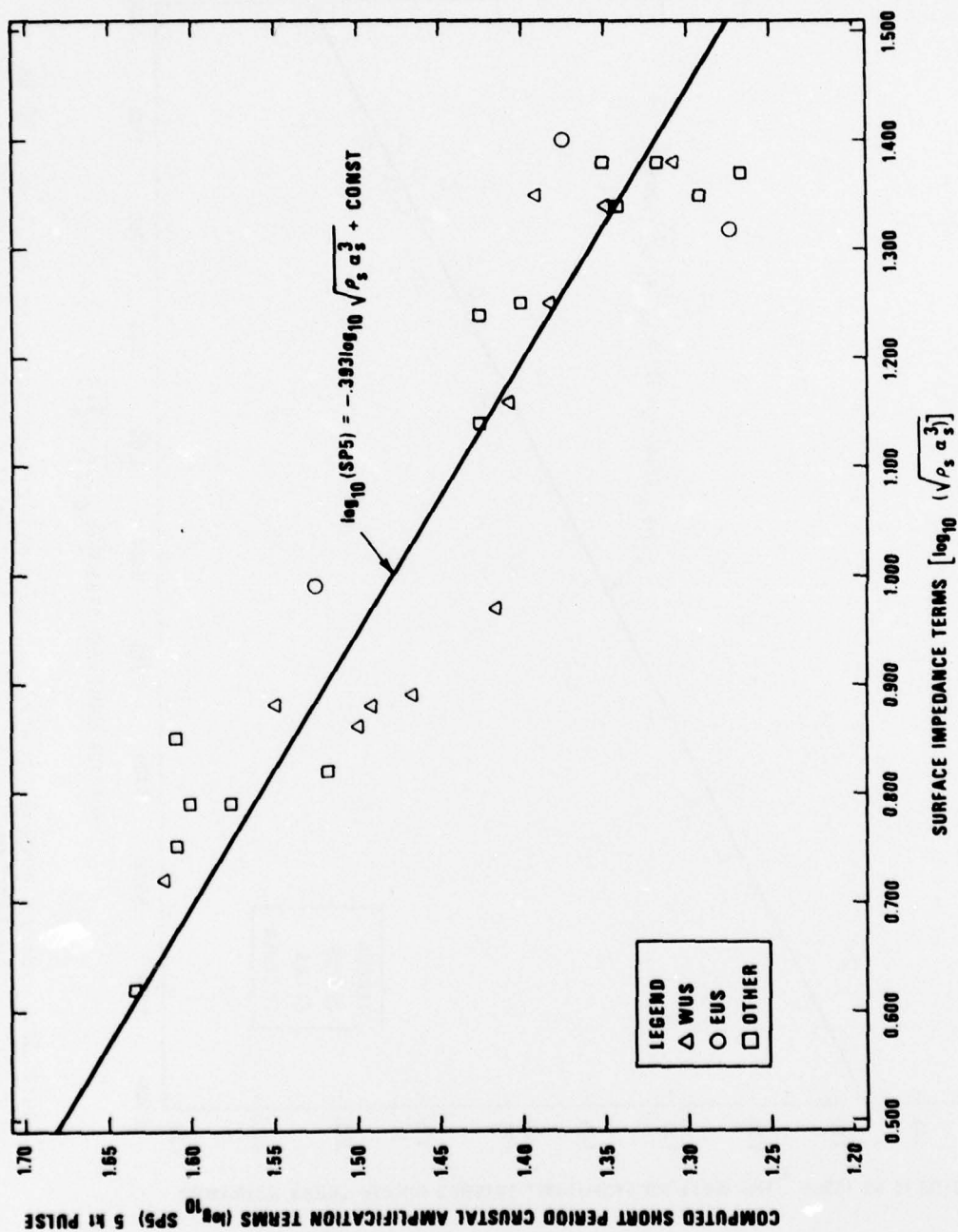
Figure 32.   Short period crustal amplification term for a pulse from a 5 kt nuclear explosion plotted against the surface acoustic impedance term. Least squares regression line is drawn through the points.

-56-

determining crustal amplification in our models. The scatter reflects the deviation between amplification due solely to surface acoustic impedances and the exact calculation of response. The scatter relative to a simple linear dependence is small. This suggests that in most cases knowledge of $\sqrt{\rho_s \alpha_s^3}$ is sufficient to approximate the theoretical crustal response. The points belonging to the EUS and WUS or third category populations are mixed together in these plots, showing that all of these groups cover a similar range in crustal amplification terms, or $\log_{10}(\sqrt{\rho_s \alpha_s^3})$. Since energy $E \sim A^2 \rho \alpha^3$, then in a slowly varying medium where energy is concerved $\log A \sim -1.0 \log \sqrt{\rho \alpha^3}$. Our calculated regression slopes of 0.327 and 0.393 reflect the fact that the influence of deeper layers is being felt on the low-frequency portions of the signal, and that for low $\rho_s \alpha_s^3$ much of the energy is reflected before it reaches the surface.

As the next step in our analysis we tried to examine the relationship between the magnitude residuals m_b^{SP} and m_b^{LP} of Booth, Marshall and Young (1974) on one hand and our crustal amplification terms $\log_{10}(SP5)$, $\log_{10}(SP50)$, $\log_{10}(LP50)$, $\log_{10}(\sqrt{\rho_s \alpha_s^3})$ and t* on the other hand for the total data set.

Figures 33 and 34 show the computed crustal amplification terms $\log_{10}$ (SP5) and $\log_{10}(SP50)$ (called crustal amplification terms) plotted against the magnitude residuals SPC of Booth et al. (1974). Triangles denote stations in western North America (WUS), squares denote stations in the EUS, circles denote stations which could not be classified into either category (ADIS, HWIS and WHYK). Both figures show that the points associated with the EUS stations form a population which is almost completely separated from those of the WUS stations. The magnitude residuals are positive in the EUS (high observed magnitudes) and negative in the WUS. The points for the three stations not belonging to either category seem to group with the EUS stations. Both the EUS and WUS populations exhibit visible trends with the crustal amplification terms although there is a lot of scatter.

The surface impedance term $\log_{10}\sqrt{\rho_s \alpha_s^3}$ was also plotted against the magnitude residuals in Figure 35. Since this quantity was shown to be highly correlated with the crustal amplification terms the distribution of

-57-
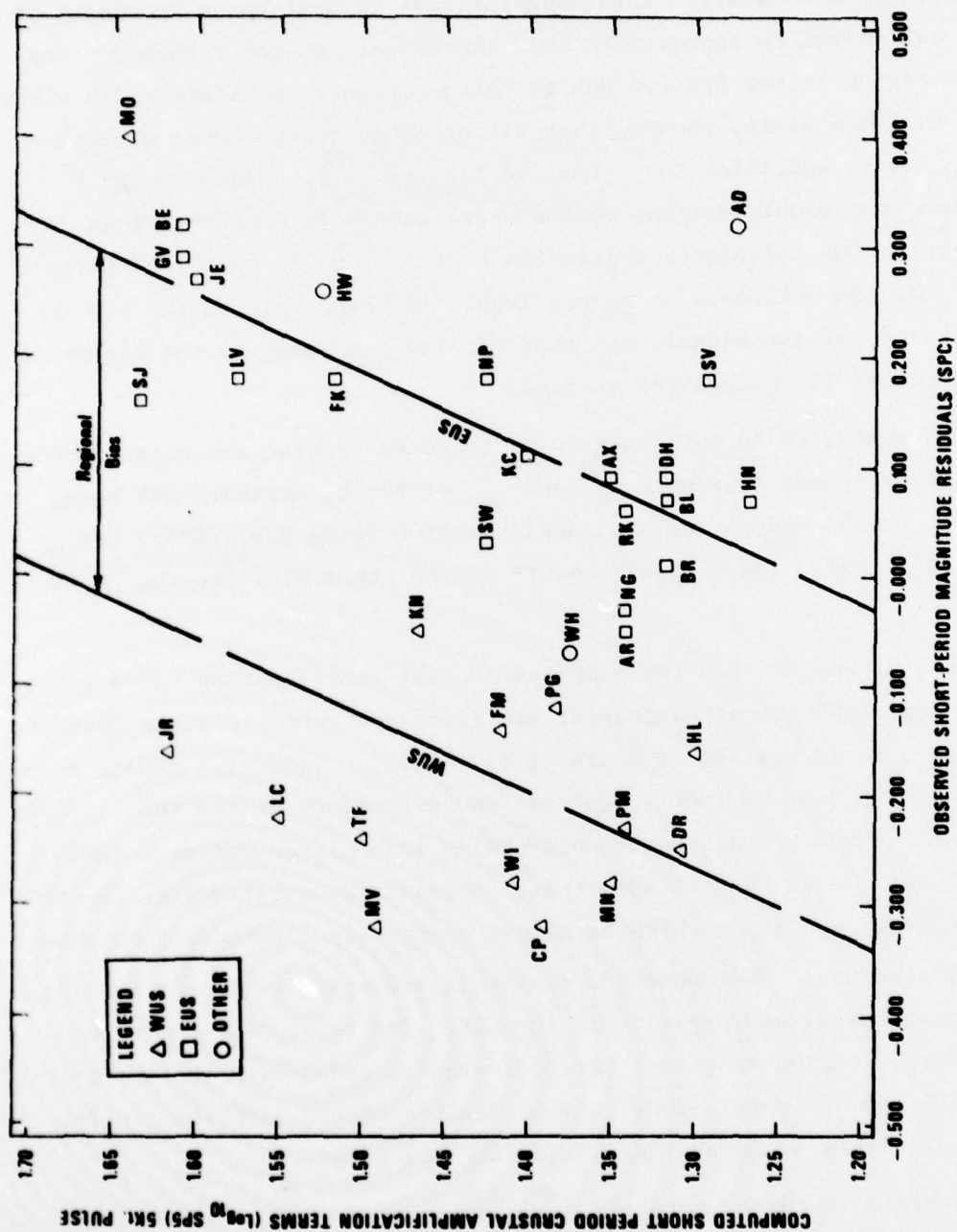
Figure 33. Short period crustal amplification term for a pulse for a 5 kt
nuclear explosion plotted against short period magnitude resid-
uals of Booth et al. (1974). Regression lines for the EUS and
WUS populations are drawn separately. Regional magnitude bias
is shown on the top of the figure.
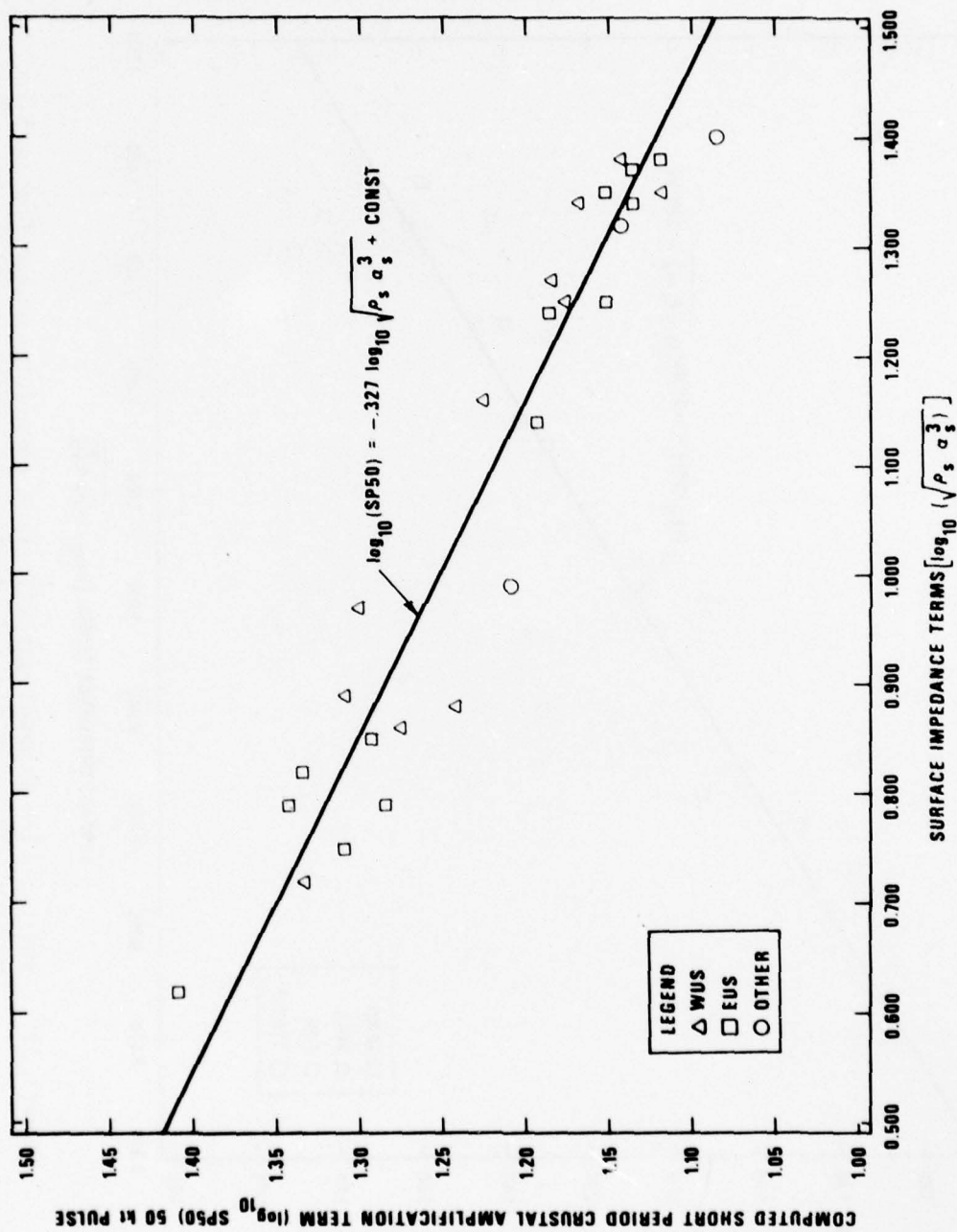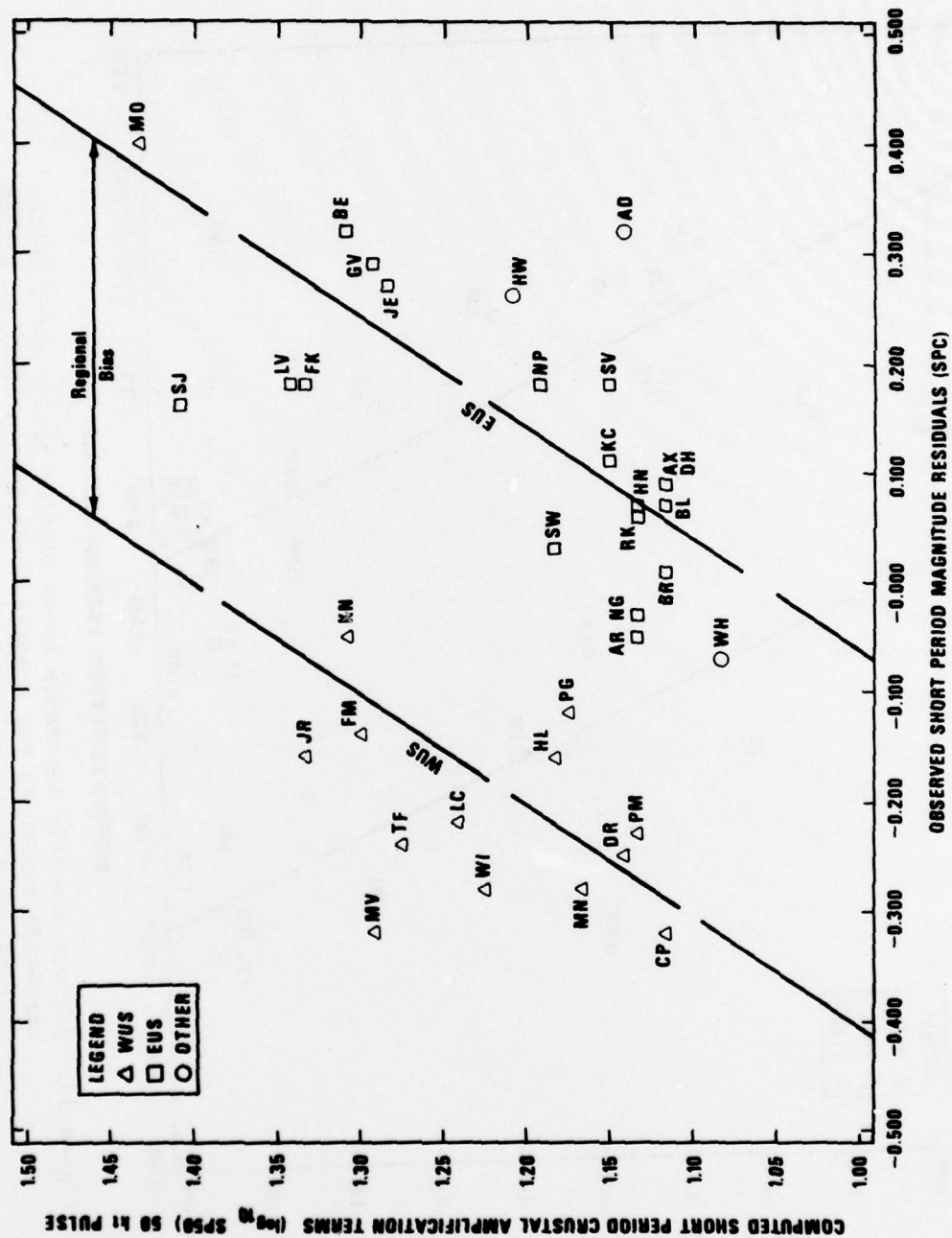
Figure 34. Short period crustal amplification term for a pulse for a 50 kt nuclear explosion plotted against short period magnitude residuals of Booth et al (1974). Regression lines for the EUS and WUS populations are drawn separately. Regional magnitude bias is shown on the top of the figure.
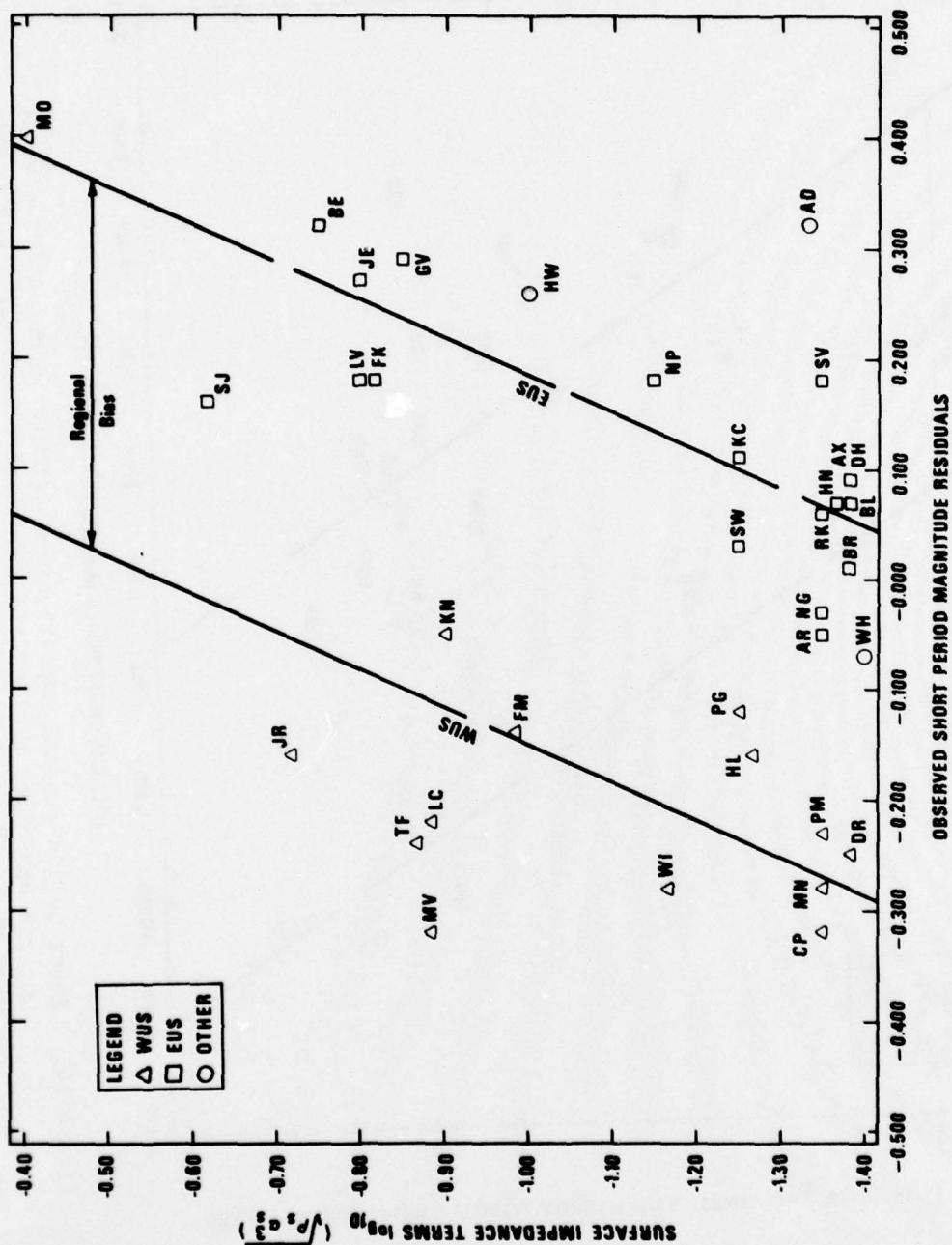
Figure 35. Surface acoustic impedance terms plotted agains short period magnitude residuals for a pulse for a 5 kt nuclear explosion plotted against the short period magnitude residuals of Booth et al. (1974). Regression lines for the EUS and WUS populations are drawn separately. Regional magnitude bias is shown on the top of the figure.

the points is very similar to those seen in the two previous figures.

In Figures 33-35 we also plotted the separate EUS and WUS lines derived by regression between the short period magnitude residuals and crustal amplification terms or surface impedance terms, respectively. These lines are based on a regression analysis described later in this report. The shift between the two lines represents an average EUS-WUS magnitude bias for the station networks used by Booth et al. (1974).

An anomalous point is MOID, which seems to group with the EUS stations due to its +0.4 residual as given by Booth et al. (1974). This station is located in a missile silo on unconsolidated silty-clayey deposits. In computing the crustal amplification, we assumed a compressional velocity of 1.5 km/sec for the surface material. Although this figure is quite low, it could be even lower. Attempts to move this point into the WUS population by lowering the velocity failed. Probably the difference reflects the effects of the dense missile silo on the silt "spring". However, without more detailed spectral analysis of this station we cannot reject the hypotheses that beneath MOID is a Q structure characteristic of the EUS or that a powerful focusing effect due to non-plane-parallel layers is operative.

To derive the foregoing regression lines we set up the following three linear hypotheses to evaluate the relative dependence of the short period magnitude residuals Δm_b^{SP} of Booth et al. (1974), on the crustal amplification terms $\log_{10}(SP5)$, $\log_{10}(SP50)$, and quantity $\log_{10}\sqrt{\rho_s\alpha_s^3}$; and on t* which is taken as .2 for EUS and .45 for WUS.

1) $m_b^{SP} = a + b \log_{10}(SP5) + ct*$

2) $m_b^{SP} = a + b \log_{10}(SP50) + ct*$

3) $m_b^{SP} = a + b \log_{10}\sqrt{\rho_s\alpha_s^3} + ct*$

The three stations not belonging to either the EUS or WUS are disregarded in this analysis. The coefficient of t* is expected to be about $-\pi f/Ln(10) = -1.36$ for 1 Hz waves. The coefficient is expected to be 1.0 for SP5 and SP50 if the calculations of crustal differential response are performing on the average as expected and if the assumed source spectrum is representative of the earthquakes used to determine m_b^{SP}. For $\log_{10}\sqrt{\rho_s\alpha_s^3}$ we

-61-

would expect a value for b of roughly 0.3 to 0.4 considering the results of Figures 31 and 32 where, for example, $\log(SP50) = -.327 \log\sqrt{\rho_s \alpha_s^3}$. The hypotheses also assign a common slope of b for both EUS and WUS populations in each case. The quantity "a" is designed to absorb all multiplicative factors, which cancel when magnitude differences are considered.

Table III shows the results of statistical analyses. The quantities shown are: the linear regression coefficients a, b, and c for the three hypotheses with their 95% confidence limits; the percentage of total variance explained by each individual variable crustal amplification and t*, and by their linear combination; and the residual (unexplained) error terms.

The table shows that the hypotheses using both variables can account for 70-75% of the total variance in magnitude residuals Δm_b^{SP}. The coefficients "b" are different from zero at the 95% confidence interval showing that crustal amplification is important in determining Δm_b^{SP}, although by itself it accounts for only about one-tenth of the total variance. The t* effect coefficient "c" is also significantly different from zero, accounting for more than one-half of the total variance. The coefficient "c" ranges between -1.25 and -1.35 which is very close to the value -1.36 quoted above.

The product $c\delta t^*$ is theoretically equal to $[\pi f/Ln(10)]\delta t^*$. With $\delta t^* =$ .25 we found for SP50 c = 1.35 which implies f = 1. Had we chosen $\delta t^* = .17$ (Der et al., 1977) c would have become 1.36 x .25/.17 = 2.00 which would imply f = 1.0 x .25/.17 = 1.47. Through March 1978 the mean values of 1/T at RKON and OB2NV were 1.49 Hz and 1.12 Hz respectively. The mean frequency of 1.3 Hz is in fair agreement with 1.47 considering the approximate nature of the frequency estimation, our lack of knowledge of the earthquake source spectra (which influence the amplitude and period differences to a small degree), and the approximate nature of the mathematical argument which is implicitly being carried out in the spectral domain instead of the more relevant time domain. The mean EUS-WUS Δm_b^{SP} differential in observed magnitudes implied by our values of c ranges between .34 to .31 magnitude units. The value of the coefficient b for Hypothesis 3 is smaller since the surface impedance term varies over a wider range than the crustal amplification terms. It is also significant that b is close to unity for the 50 kt pulse which indicates that

-62-

TABLE III

Hypothesis 1

Independent variables used	Residual rms error (m_b units)	Percentage of total variance explained
$\log_{10}(SP5)$, t^*	.12	70
$\log_{10}(SP5)$	.20	13
t^*	.15	53

Regression coefficients

$a = -.64$

$b = .72 \pm .37$ (95% conf.)

$c = -1.25 \pm .34$ (95% conf.)

Implied EUS-WUS regional magnitude bias
$\Delta m_b = .31$

Hypothesis 2

Independent variables used	Residual rms error (m_b units)	Percentage of total variance explained
$\log_{10}(SP50)$, t^*	.11	.74
$\log_{10}(SP50)$	.20	.10
t^*	.15	.53

Regression coefficients

$a = -.83$

$b = 1.03 \pm .43$ (95% conf.)

$c = -1.35 \pm .32$ (95% conf.)

Implied EUS-WUS regional magnitude bias
$\Delta m_b = .34$

Hypothesis 3

Independent variables used	Residual rms error (m_b units)	Percentage of total variance explained
$\log_{10}(\sqrt{\rho_s \alpha_s^3})$, t^*	.11	.75
$\log_{10}(\sqrt{\rho_s \alpha_s^3})$	.20	.12
t^*	.15	.53

Regression coefficients

$a = .80$

$b = .35 \pm .14$ (95% conf.)

$c = -1.33 \pm .31$ (95% conf.)

Implied EUS-WUS regional magnitude bias
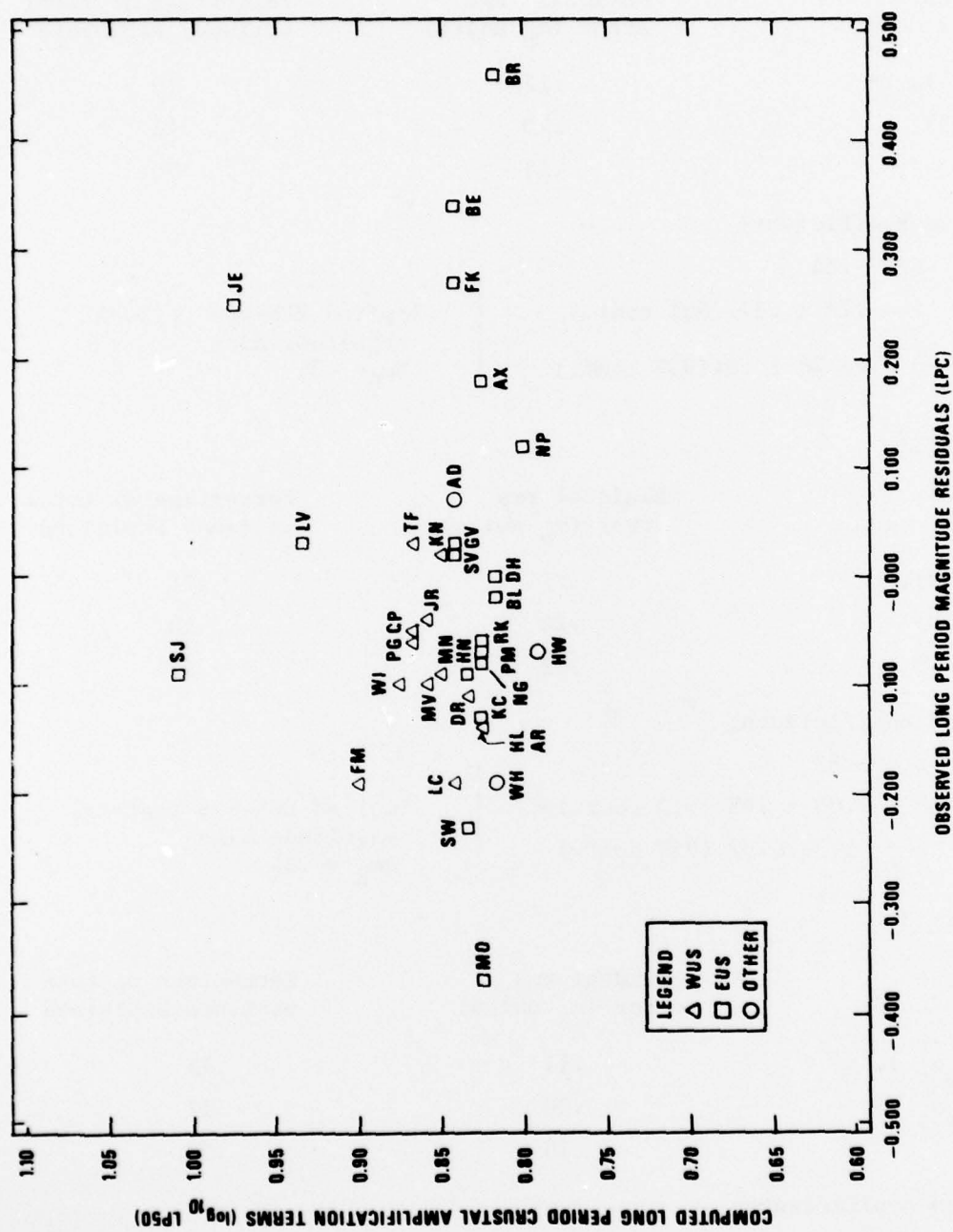$\Delta m_b = .33$

Figure 36. Long period crustal amplification terms plotted against the long period magnitude residuals of Booth et al. (1974).

crustal amplification for this pulse is a proper estimator for magnitude residuals. If b were forced to a value of 1.0 in all three hypotheses, then the highest proportion of variance would be explained by Hypothesis 2. The small value of b for the 5 kt pulse shows that crustal amplification of this pulse overestimates the crustal effect. This is due, undoubtedly, to the high frequency content of this pulse.

Although a great part (up to 75%) of the total variance in Δm_b^{SP} can be explained by the combination of crustal amplification and t* in all three hypotheses investigated, the remaining variance is not small. The remainder can be caused by factors such as the real variation in t* in both populations, imperfect crustal modelling, crustal focusing, etc. It also reflects the inherent variability of time-domain amplitude measurements well demonstrated by variation of amplitudes across LASA and NORSAR, see e.g., Klappenberger (1967), Blandford (1974), Chang and von Seggern (1977).

In Figure 36 we see that the observed variation of long-period residuals is much greater than can be explained by crustal structure, and there is no EUS-WUS separation. Evidently focusing and other effects are dominant.

Klappenberger, F. (1967). Distribution of short-period P phases over LASA, Seismic Data Laboratory Report 287, Teledyne Geotech, AD 815-580.

Blandford, R. (1974). Short period signal to noise ratio at NORSAR, SDAC-TR-74-13, Teledyne Geotech, ADA 015650.

Chang, A. and D.von Seggern (1977). A study of amplitude anomaly and m_b bias at LASA subarrays, SDAC-TR-77-11, Teledyne Geotech, Alexandria, Va.

ACKNOWLEDGEMENTS

REFERENCES

Antoine, J. and J. Ewing (1963). Seismic-refraction measurements of the Gulf of Mexico, J. Geophys. Res., v. 68, p. 1975.

Asada, T., L. T. Aldrick (1966). Seismic observations of explosions in Montana, AGU Monograph #10, The Earth Beneath the Continents, J. S. Steinhart and T. Jefferson, editors.

Båth, Marcus (1968). Mathematical Aspects of Seismology, Elsevier Publishing Company, Amsterdam.

Blandford, R. (1974). Short period signal to noise ratio at NORSAR, SDAC-TR-74-13, Teledyne Geotech, ADA 015650.

Booth, Marshall and Young (1974). Long and short-period amplitudes from earthquakes in the range 0°-114°, Geohpys. J. R. Astr. Soc., 39, 523-538.

Brune and Dorman (1963). Seismic waves in the Canadian Shield, Bull. Seism. Soc. Am., v. 53, p. 167-210.

Chang, A. and D. von Seggern (1977). A study of amplitude anomaly and m_b bias at LASA subarrays, SDAC-TR-77-11, Teledyne Geotech, Alexandria, Va.

Cram, I. H. (1961). A crustal structure refraction survey in South Texas, Geophysics, v. 26, p. 560-573.

Dainty, A. M., C. E. Keen and J. E. Blanchard (1966). Review of Geophysical evidence on the Eastern Seaboard of Canada, AGU Monograph #10, The Earth Beneath the Continents, J. S. Steinhart and T. Jefferson Smith, editors.

Der, Z. A., M. S. Dawkins, T. W. McElfresh, J. H. Goncz, C. E. Gray, M. D. Gillispie, (1977). Teleseismic P wave amplitudes and spectra at NTS and the Shoal site as compared to those observed in Eastern North America, Preliminary Report, SDAC-TR-77-9, Teledyne Geotech, Alexandria, Virginia. DDC ADA 045096

Eardley, E. J. (1951). Structural Geology of North America, 1951, Harper Bros., New York.

Evernden and Clark (1970). Study of teleseismic P. II. amplitude data, Phys. Earth Planet Interiors, v. 4, p. 24-31.

Ewing, M. W., Jardetzky, W. S., and F. Press (1957). Elastic Waves in Layered Media, McGraw-Hill Book Company, New York.

Geotech LRSM site reports, Teledyne Geotech, Garland, Texas.

Haskell, (1962). Crustal reflection of P and SV waves, J. Geophys. Res., v. 67, p. 4751-4767.

REFERENCES (Continued)

Healy, J. H. (1973). Crustal structure along the Coast of California from
    seismic-refraction measurements, J. Geophys. Res., v. 68, p. 5777- 5787.

Herrin, E. T. and J. Taggart (1962). Regional variations in P velocity and
    their effect on the location of epicenters, Bull. Seism. Soc. Am.,
    v. 52, p. 1037-1046.

Hill, D. P. and L. C. Pakiser (1966). Crustal structure between the Nevada
    Test Site and Boise, Idaho, from seismic-refraction measurements, AGU
    Monograph #10, The Earth Beneath the Continents, J. S. Steinhart and
    T. Jefferson Smith, editors.

Hill, D. P. (1969). Crustal structure of the Island of Hawaii from seismic-
    refraction measurements, Bull. Seism. Soc. Am., v. 59, p. 101-130.

Jackson, W. H., S. W. Steward and L. C. Pakiser (1963). Crustal structure in
    Eastern Colorado from seismic-refraction measurements, J. Geophys. Res.,
    v. 68, p. 5767.

Jacob, K. H. and K. Hamada (1972). The upper mantle beneath the Aleutian
    Island Arc from pure-path Rayleigh-wave disperson data, Bull. Seism.
    Soc. Am., v. 62, p. 1439-1453.

Johnson, L. R. (1965). Crustal structure between Lake Mead, Nevada and Mono
    Lake, California, J. Geophys. Res., v. 70, p. 2863-2872.

Keller, G. R., R. B., Smith, L. W. Braile (1975). Crustal structure along
    the Great Basin-Colorado Plateau trasition for seismic-refraction studies,
    J. Geophys. Res., v. 80, p. 1093-1098.

Keller, G. R., R. B. Smith, L. W. Braile, R. Heaney, and D. H. Shurbet (1976).
    Upper crustal structure of the eastern Basin and Range, northern Colorado
    Plateau and middle Rocky Mountains from Rayleigh-wave dispersion,
    Bull. Seism. Soc. Am., v. 66, p. 869-976.

Klappenberger, F. (1967). Distributuion of short-period P phases over LASA,
    Seismic Data Laboratory Report 287, Teledyne Geotech, AD 815-580.

LeBlanc, G. and R. J. Wetmiller (1974). An evaluation of seismological data
    for the Yukon Territory and the Mackenzie Valley, Can. Journal of Earth
    Sci., v. 11, p. 1435-1454.

Niazi, M. (1969). Use of source arrays in studies of regional structure, Bull.
    Seism. Soc. Am., v. 59, p. 1631-1643.

Pakiser, L. C. and J. S. Steinhart (1964). Explosion seismology in the Western
    Hemisphere, Research in Geophysics, V. 2, MIT Press.

Pakiser, L. C. and I Zietz (1965). Transcontinental crustal and upper mantle
    structure, Rev. Geophys., v. 3, p. 505-520.

REFERENCES (Continued)

Richard, T. C. and D. J. Walker (1959). Measurement of thickness of the earth's crust in the Alberta plains of Western Canada, Geophysics, v. 24, p. 262-64.

Stewart, S. W. (1968). Crustal structure in Missouri by seismic-refraction methods, Bull. Seism. Soc. Am., v. 58, p. 291-323.

Toppozada, T. R. and A. R. Sanford (1976). Crustal structure in central New Mexico interpreted from the Gasbuggy explosion, Bull. Seism. Soc. Am., v. 66, p. 877-886.

Tryggvason, E. and B. R. Qualls (1967). Seismic-refraction measurements of crustal structure in Oklahoma, J. Geophys. Res., v. 72, p. 3738-3740.

White, W. R. H. and J. C. Savage (1965). A seismic-refraction and gravity survey of the Earth's crust in British Columbia, Bull. Seism. Soc. Am., v. 55, p. 463-486.

Woeber, A. F. and J. O Pennhollow (1975). Depth prediction from velocity profiles on the Texas Gulf Coast, Geophysics, v. 40, p. 388-398.

Woolard, G. P. (1959). Crustal structure from gravity measurements, J. Geophys. Res., 64(2), 1525-1544.